

Controls and evolution of facies patterns in the Upper Barremian–Albian Levant Platform in North Sinai and North Israel

MARTINA BACHMANN*, JOCHEN KUSS & JENS LEHMANN

Department of Geosciences, Bremen University, P.O. Box 330440, 28334 Bremen, Germany

**Corresponding author (e-mail: Bachmann@uni-bremen.de)*

Abstract: The Upper Barremian–Albian Levant Platform was studied in North Sinai and Israel (Galilee and Golan Heights) by bio- and lithostratigraphy, facies analyses, and sequence stratigraphy. Integrating shallow-marine benthic foraminifera (mainly orbitolines), ammonite, and stable isotope data resulted in a detailed stratigraphic chart. Transects across the shallow shelf in both regions are based on facies analysis and form the basis for depositional models. In both transects five platform stages (PS I–V) were identified, which differ significantly in their stratigraphic architecture, mainly controlled by local tectonics, climate and second-order sea-level changes. In North Sinai, a transition from a shallow-shelf that is structured by sub-basins through a homoclinal ramp into a flat topped platform is recognized, while the sections in North Israel show a transition from a homoclinal ramp into a fringing platform. Local normal faults influenced the depositional architecture of the Upper Barremian–Lower Aptian strata in North Sinai and were attributed to syn-rift extensional tectonics. Four second-order sequence boundaries were identified, bounding Mid-Cretaceous Levant depositional sequences. These well-dated second-order sequence boundaries are MCL-1 (Late Barremian), MCL-2 (earliest Late Aptian), MCL-3 (Lower Albian), and MCL-4 (Late Albian). The sea-level history of the Levant Platform reflects the Late Aptian–Albian global long-term transgression, while the second-order sea-level changes show good correlation with those described from the Arabian plate.

The Late Barremian–Albian Levant Platform is an ideal case study for studying platform development in a setting of global long-term sea-level change, climate variation, and geodynamics. The platform was located at the northern rim of the North African/Arabian plate and the southern border of the Tethyan Ocean, respectively (Fig. 1a). Extending from southern Lebanon to northern Egypt the Levant Platform strikes out in a narrow stripe parallel to the recent coastline (Saint-Marc 1974; Braun & Hirsch 1994; Kuss & Bachmann 1996; Rosenfeld *et al.* 1998). Its central part was studied in Israel (Galilee and Golan Heights) and its south-western part in North Sinai, both characterized by good exposures (Fig. 1b, c). During the Late Barremian–Albian about 500 m of shallow marine deposits accumulated on the Levant Platform.

During the Mesozoic, the region was characterized by extensional and compressive tectonical processes related to the opening and closure of the Neotethys (e.g. Keeley 1994; Hirsch *et al.* 1995; Stampfli & Borel 2002; and other papers in this volume) forming the main tectonical structures such as the Syrian Arc fold belts and the Dead Sea Transform (DST). However, the analysed interval represents a consistent platform succession deposited since the Late Barremian. This interval has been interpreted to be deposited in a post-extensional setting during mid-Cretaceous

transgression and indicating relative tectonical quiescence before the onset of Late Cretaceous compression (Moustafa & Khalil 1990; Hirsch *et al.* 1995; Kuss & Bachmann 1996).

Most former studies concentrate on small areas and/or selected stratigraphical or palaeontological parameters. Litho- and biostratigraphical concepts of the Lower Cretaceous of Galilee and the Golan Heights are summarized in Rosenfeld & Hirsch (2005) and Bachmann & Hirsch (2006); tectonic concepts are summarized in Flexer *et al.* (2005) and Gilat (2005). Stratigraphical subdivisions of the Lower Cretaceous of the Sinai, are mainly based on Said (1971) and Bartov & Steinitz (1977). Younger interpretations include facies, stratigraphic and sedimentological data (Aboul Ela *et al.* 1991; Askalany & Abu-Zeid 1994; Bachmann & Kuss 1998; El-Araby 1999; Steuber & Bachmann 2002; Bachmann *et al.* 2003). Only few studies document marine Barremian–Lower Aptian sediments in North Sinai (Arkin *et al.* 1975; Morsi 2006; Abu-Zied 2007, 2008).

In the present paper, we summarize various stratigraphical data with respect to a consistent correlation of various lithological units in the area and add new data from the Barremian–Lower Aptian succession of North Sinai. The methodology includes bio- and isotope stratigraphy, the interpretation of sedimentological structures in the field,

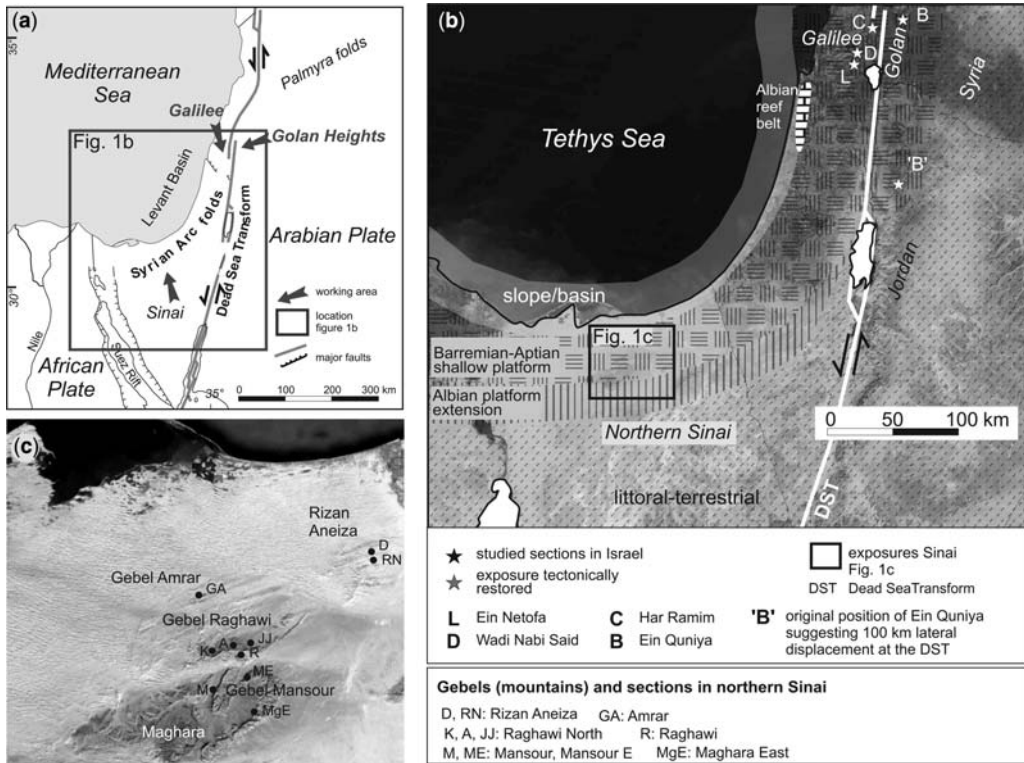


Fig. 1. Location of the study area. (a) Tectonic map, simplified after Garfunkel (1998) with the location, the two study areas in North Sinai and northern Israel (Galilee and Golan Heights) straddling the DST fault. (b) Aptian–Albian palaeoenvironmental map of the Levant Platform, modified from Rosenfeld *et al.* (1998) and supplemented by results from North Sinai indicating the extension of the shallow platform facies belts. (c) Gebel (mountains) examined in North Sinai indicated on a satellite map. 'B' indicates the tectonically restored position of the Golan Heights section B, when assumed the lateral movement of 100 km as indicated, for example by Garfunkel & Ben-Avraham (1996).

small-scaled geological mapping, and microfacies analysis. Our interpretations are focused on facies reconstructions and long-term, second-order, sea-level changes within a high-resolution stratigraphical frame. Moreover, we estimated the climatic and tectonic influences on the sedimentation. The data allow us to reconstruct and interpret the varying Late Barremian–Albian shelf geometry, as well as the timing and interpretation of the platform development. In this respect syn-depositional tectonic processes were determined, which were previously unknown.

These data are interpreted, allowing the detailed timing of the Late Barremian–Albian succession. This results in an evaluation of the facies, long-term local and regional second-order sea-level changes, and climate framework, characterizing the complex sedimentary system of the Levant Platform. Furthermore, the data allow us to reconstruct and interpret the varying Late Barremian–Albian shelf geometry. In this respect,

the paper is a review. Together with new data, especially from the Barremian–Lower Aptian succession of North Sinai, the dataset allows the interpretation of the platform development.

Most former studies concentrate on small areas and/or selected stratigraphical or palaeontological parameters. Litho- and biostratigraphic concepts of the Lower Cretaceous period of Galilee and the Golan Heights are summarized in Rosenfeld & Hirsch (2005) and Bachmann & Hirsch (2006), tectonic concepts are summarized in Flexer *et al.* (2005) and Gilat (2005).

Stratigraphic subdivisions of the Lower Cretaceous of the Sinai are mainly based on Said (1971) and Bartov & Steinitz (1977). Younger interpretations include (Abou Ela *et al.* 1991; Askalany & Abu-Zeid 1994; Bachmann & Kuss 1998; El-Araby 1999; Steuber & Bachmann 2002; Bachmann *et al.* 2003). Only few studies document marine Barremian–Lower Aptian sediments in North Sinai (Arkin *et al.* 1975; Morsi 2006; Abu-Zied 2007).

Geological framework

The Levant Platform developed at the northern passive continental margin of the African–Arabian plate close to the plate boundary with the Anatolian plate. The tectonical pattern in the Eastern Mediterranean Levantine region has important influence on the Cretaceous platform development characterized by this position at the triple junction of the African, Arabian, and Anatolian plates (Flexer *et al.* 2005). The Early Mesozoic opening of the Neotethys generated an east–west striking rift system with subsiding areas and thus created the Levant Basin at the northeastern edge of the African–Arabian plate (Keeley 1994; Hirsch *et al.* 1995; Garfunkel 1998; Flexer *et al.* 2005). The shallow-marine Levant Platform formed at the southeastern passive margin of the Levant Basin trending in a narrow strip parallel to the Mediterranean coastline from Lebanon and Syria through Israel to North Sinai, Egypt (Garfunkel 1998). The breakup of the Levant Platform commenced with the Late Coniacian–Palaeogene inversion of extensional faults (Flexer *et al.* 2005).

In northern Israel, the initial ramp geometry of the Early Cretaceous Levant Platform developed into a flat-topped platform in the Early Aptian (Bachmann & Hirsch 2006). In the Albian it is saddled by the formation of fringing rudist-reefs at the shelf break (Sass & Bein 1982; Ross 1992). In North Sinai, the initial Upper Barremian–Lower Aptian platform is not yet analysed. The Upper Aptian–Lower Albian platform geometry is described as a distally steepened ramp (Bachmann & Kuss 1998). The region in between North Sinai and northern Israel is described as a gradual shallow–deep transition (Rosenfeld *et al.* 1998) known only from the subsurface (Rosenfeld & Hirsch 2005).

The investigated sections and lithostratigraphical concepts

In northern Israel/Galilee and the Golan Heights, most outcrops are located along strike–slip faults orientated parallel to the DST fault and in asymmetric Syrian Arc anticlinal structures (Flexer *et al.* 2005; Gilat 2005). In North Sinai, several anticlinal Syrian Arc structures form good outcrop conditions (Moustafa & Khalil 1990).

Owing to the regional differentiated nomenclature, with a high number of units, members and formations, we compile standard sections for the two platform edges composed from several sections in both regions (Fig. 1).

Galilee/Golan. We follow the lithostratigraphical subdivisions of the Cretaceous succession in the Golan Heights and Galilee established by Eliezeri

(1965) and modified by Rosenfeld *et al.* (1995), while additionally distinguishing a new member (Fig. 2). The terrestrial sandstones at the base of the succession are known as the Hatira Formation and occur in the subsurface of northern Israel (Rosenfeld *et al.* 1998). The overlying marine succession is subdivided into five formations: Nabi Said (ooid-rich limestones), Ein el Assad (limestones and subordinated marlstones), Hidra (sandstones, marlstones, and few limestone beds), Rama (limestones and marlstones), and Yagur (limestones and dolomites) (Fig. 2). The studied succession is 440 m thick; the standard section is based on three sections studied in Galilee (Har Ramin, Rama and Ein Netofa) and one on the Golan Heights (Ein Quniya) (Bachmann & Hirsch 2006), (Fig. 1). Hence outcrops of marine Lower Cretaceous sediments are generally rare in Galilee and the Golan Heights, two sections (Har Ramin/Galilee and Ein Quniya/Golan Heights) comprise the entire 440 m thick Upper Barremian–Albian succession. Weathering profiles, bedding surfaces, sedimentary structures, stratigraphical, and facies interpretation are described in Bachmann & Hirsch (2006).

North Sinai. We use the lithostratigraphical subdivision of the Upper Barremian–Albian succession of North Sinai of Said (1971), applied in current geological maps (Fig. 2). The platform succession starts above terrestrial sandstones (Malha Formation) with a limestone, dolomite, and marlstone alternation characterized by detrital influence (lower Rizan Aneiza Formation). Sandstone, marlstone, limestone, and dolomite alternations with deltaic influence above represent the upper Rizan Aneiza Formation; the subsequent succession of limestones and dolomitic marlstones without considerable siliclastic input was related to the Halal Formation. The thickness of individual sections varies greatly, depending on their palaeogeographical position. From south to north, the thickness of the lower part of the Rizan Aneiza Formation varies from 0 to 170 m and from 120 to 250 m for the upper part of the Rizan Aneiza Formation. The lower Halal Formation studied at Gebel Mansour reaches 220 m.

The Upper Barremian–Upper Albian succession of North Sinai was studied in five anticlinal structures, comprising the following Gebels: Amrar, Rizan Aneiza, Raghawi, Mansoura, and southeastern Maghara (Fig. 1c). Within this frame, the Raghawi section (A) describes a proximal setting of the lower Rizan Aneiza Formation (Upper Barremian–lower Upper Aptian) (Fig. 2), while the Amrar section (GA) shows a more distal expression of the same interval. One Rizan Aneiza section (D) includes the Lower/Upper Aptian boundary, while the eastern Maghara section

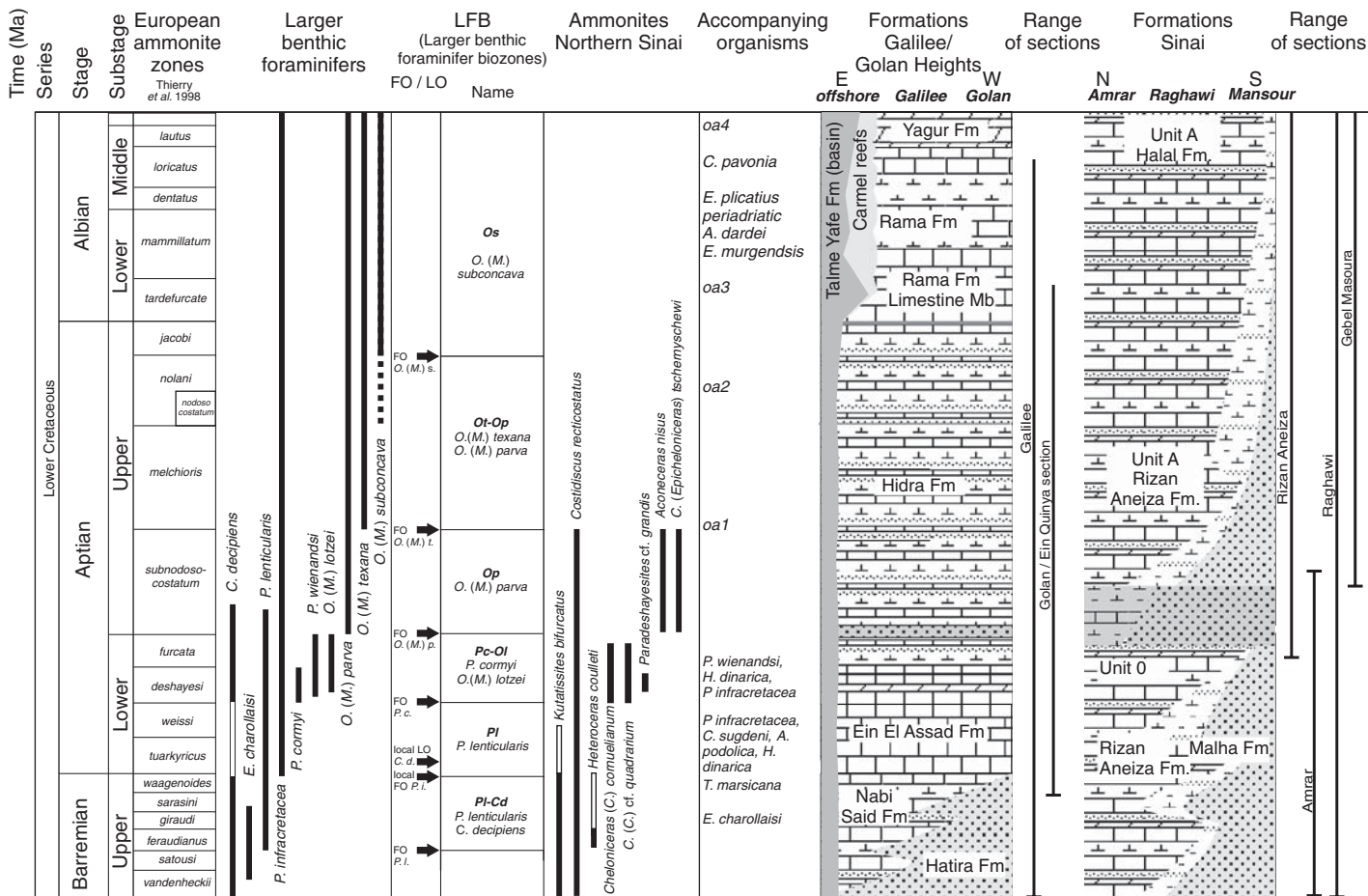


Fig. 2. Biostratigraphic subdivision of the Upper Barremian–Albian ranges of the LFBs, timing of the lithostratigraphical formations and members and ranges of the sections. The ranges of the most important benthic foraminifers and the ammonites are compiled from several authors (see text) and arranged in the chronostratigraphic framework of Ogg *et al.* (2004). Accompanying organisms are taken from Bachmann & Hirsch (2006) and Bachmann *et al.* (2003). ‘oa’ refers on ostracod assemblages observed in North Sinai (Bachmann *et al.* 2003).

(MgE) completes the Lower–Middle Albian succession (upper Rizan Aneiza Formation) to the SE.

These sections are summarized and span a 40 km wide transect from the distal Amrar anticline in the NW to the proximal Maghara structure in the SE (Fig. 1c). Eight sections from the upper Rizan Aneiza and lower Halal formations (Upper Aptian–Albian) were presented in former publications (Bachmann & Kuss 1998; Bachmann *et al.* 2003); three of them are added in this work (Fig. 1c) to illustrate facies and sequence stratigraphy.

Methods

For the North Sinai sections, weathering profiles, bedding surfaces, sedimentary structures, and facies characteristics are documented. Sample distances of the limestone intervals are usually less than 1 m and may be higher in the marlstone and sandstone-dominated intervals. Stratigraphy and facies were analysed by using field data, thin sections, ammonite findings and washed samples, and stable isotopes analyses required powdered samples.

Biostratigraphy. Biostratigraphy is based on benthic foraminifers (mainly orbitolinids) and ammonites. The orbitolinid distribution (taxonomy according to Schroeder 1975) allows the definition of six larger benthic foraminifera biozones (LFBs), of which five are originally defined on the first occurrence and/or last occurrence (FO/LO) of the eponymous species in the Galilee/Golan area (Fig. 2, Bachmann & Hirsch 2006). We compare our biostratigraphic data with those of the northern Tethys (Schroeder & Neumann 1985; Arnaud-Vanneau 1998; Arnaud *et al.* 1998; Bernaus *et al.* 2002; Schroeder *et al.* 2002; Conrad *et al.* 2004) and the Middle East (Saint-Marc 1974; Simmons & Hart 1987; Simmons 1994; Simmons *et al.* 2000), and integrate the LFBs with the chronostratigraphy of Hardenbol *et al.* (1998a, b) and Ogg *et al.* (2004) also considering calcareous algae following Bachmann & Hirsch (2006).

Ammonites from nearly all sections in North Sinai are determined and allow comparison with the Tethyan ammonite zonation (e.g. Rawson *et al.* 1999; García-Mondéjar 2009) and to correlate the LFBs with the ammonite range charts. The stratigraphical framework of the Upper Aptian–Albian succession additionally comprises the ranges of ostracods and rudists and is supported by graphical correlation (Bachmann *et al.* 2003).

Stable isotopes. A total of 69 bulk rock samples were analysed for carbon isotopes from the Upper Barremian–Lower Aptian of section A (Fig. 1c), North Sinai. To avoid diagenetic alteration, all samples were selected from the micritic parts of

the limestones. The stable isotope composition was measured using a Finigan mass spectrometer at Research Center Ocean Margins (RCOM) Bremen. The results are expressed in the common δ -notation in per mille relative to PDB (PeeDee belemnite) standard.

Facies analysis. The thin-section analysis includes the determination of the relative abundance of skeletal and non-skeletal components, matrix composition as well as grain size. We distinguish between abundant, common, and rare occurrence of the components. Microfacies types (MFT) were distinguished according to their texture, matrix, and components, added to data observed already in the field such as lithology, bedding patterns terrigenous input, and abundance of ferruginous ooids and macrofossils. The microfacies types are summarized in facies zones (FZ), which include microfacies types occurring in similar environments.

Palaeoenvironment reconstruction and sequence stratigraphical interpretation. Within the stratigraphic framework, the combination of small-scale mapping, log-correlation, and microfacies data (including a review of further data) results in palaeoenvironmental maps of North Sinai to northern Israel for five time slices. Despite the limited number of sections, the general platform geometries could be reconstructed. The stratigraphical correlation of all sections within the two analysed depositional areas allows the interpretation of the platform architecture as a function of accommodation, sediment supply, and production. Lateral and vertical facies changes reflect water-depth and palaeoenvironment variations, which were compared between the Galilee/Golan Heights and Sinai and are interpreted in considering sea-level history and tectonic development. Second-order sequences are reflected by lateral and vertical facies distribution patterns. Sequence stratigraphical terminology as originally developed for third-order sequences (Vail *et al.* 1991) is used herein for the second-order cycles. Our tectonic interpretations benefit from the models given by Moustafa (2010).

Stratigraphy

The stratigraphical subdivision is focused on biostratigraphy supplemented by stratigraphical interpretations of $\delta^{13}\text{C}$ curves. Biostratigraphy of the Upper Barremian–Lower Aptian from northern Sinai on ammonites and orbitolinids is integrated with carbon isotope measurements, summarized in Figure 2. This chart allows the comparison of the studied shoal-water environments with stratigraphical subdivisions of basinal settings and platform settings. Subdivision of the Upper

Aptian–Albian is based on orbitolinids, ostracods, rudists and ammonites, data based mainly on Bachmann *et al.* (2003). The stratigraphical interpretation of the sections is shown in Figure 3a, b.

Benthic organisms

The abundant orbitolinids in all sections and their wide range of habitats (lagoonal to deeper platform areas, e.g. Pittet *et al.* 2002) allow the subdivision of the Upper Barremian–Middle Albian succession into five larger benthic foraminifer biozones (LFBs). From base to top these are: **PI–Cd** *Palorbitolina lenticularis*–*Choffatella decipiens*, **PI** *P. lenticularis*, **Pc–Ol** *Praeorbitolina cormyi*–*Orbitolina (Mesorbitolina) lotzei*, **Op** *O. (M.) parva*, **Ot–Op** *O. (M.) texana*–*O. (M.) parva* in the Golan Heights/Galilee area (Bachmann & Hirsch 2006). The occurrence of *Eopalorbitolina charollaisi*, which is not younger than Late Barremian (Clavel *et al.* 1995; Arnaud *et al.* 1998; Conrad *et al.* 2004), in North Sinai (Amrar section) and Galilee (Ein Netofa area), confirms the Late Barremian age for the LFB **PI–Cd**. This stratigraphical frame is extended by a sixth LFB (**Os**) occurring in North Sinai, which is characterized by the first occurrence (FO) of *O. (M.) subconca* (Fig. 2). LFB (**Os**) ranges from uppermost Aptian to Albian and coincides with the FO of *O. (M.) subconca* in the latest Aptian of the Tethyan realm (Castro *et al.* 2001; Schroeder & Neumann 1985) and in the Middle East (Simmons *et al.* 2000). The upper boundary of LFB (**Os**) is placed at the FO of *Orbitolina (C.) corbarica* in North Sinai (Bachmann *et al.* 2003), coinciding with the Albian/Cenomanian boundary. The orbitolinid-distribution of the Upper Barremian–Lower Aptian sections in Sinai is presented in Figure 3. Ranges of the LFBs for Golan Heights–Galilee and the younger sediments of Sinai are shown in Figs 3 and 4.

Ammonites

Ammonites were sampled in North Sinai, at Gebel Raghawi (section A) and three sections 3 km east and west of section A (R1, K and JJ, Fig. 1c), which can be directly correlated by characteristic marker beds. Additionally, a few ammonites were sampled in the Rizan Aneiza area.

The Upper Barremian–Lower Aptian of these sections contains rare heteromorph ammonites, including heteroceratids. One of these, *Kutatissites bifurcatus* (section R), is an index species for the Upper Barremian, but it ranges into the Lower Aptian (Aguado & Company 1997). *Heteroceras couletti*, occurring at Gebel Raghawi, is known from the Upper Barremian of southern France (Delanoy 1997; Delanoy & Ebbo 2000). This

species occurs first in the uppermost *Hemihoplites feraudianus* Zone and ranges up to the lower *Imerites giraudi* Zone (middle Late Barremian, Fig. 2) (Delanoy 1997).

Chelonicer (*Chelonicer*) and *deshayesitids* are the most common ammonites of the Lower Aptian in North Sinai. *Chelonicer* (*C.*) *cornuelianum* and *Chelonicer* (*C.*) cf. *quadrarium* (section JJ, Raghawi,) are widely distributed taxa. *C. (C.) cornuelianum* is known from the Boreal of southern England (Casey 1962) and from Spain, Colombia, Texas, Georgia and Turkmenistan. *C. (C.) quadrarium* is known from southern England and Colombia (Kotetishvili 1970; Young 1974; Lillo Bevia 1975; Sharikadze *et al.* 2004). These cheloniceratids indicate the *Deshayesites deshayesi* and *Tropaeum bowerbanki* zones of the Boreal zonation [sensu Casey *et al.* (1998), the *T. bowerbanki* Zone, corresponding to the *D. furcata* zone in the present paper, late Early Aptian, Fig. 2]. In the same interval *Pseudohoplites matheroni* occurs, that is of limited use for biostratigraphy. The base of the Upper Aptian is characterized by an *Aconecer* *nisus* found at northern Raghawi (sections R and A), a species that is also common in Russia and northern Germany (Kemper 1995; Mikhailova & Baraboshkin 2002). *A. nisus* is accompanied by *Chelonicer* (*Epicheloniceras*) *tshernyschewi*, which is described from the Boreal in the equivalent of the *Chelonicer* (*Epicheloniceras*) *subnodosocostatum* zone (early Late Aptian, Fig. 2).

Stable isotopes

Carbon isotope values vary between -1.0‰ and 3.5‰ (Fig. 3). While the Upper Barremian–lowermost Aptian values display a gradually increase from 0.5 to 3.0‰ (interrupted by a small drop only), the upper part of the Lower Aptian succession is characterized by a distinct drop (to -1‰), a subsequent increase (to 3.5‰), and a drop (to 1‰) of the $\delta^{13}\text{C}$ values until the Lower/Upper Aptian boundary (Fig. 3). Although, the measured data show general lighter values than those from pelagic sections (e.g. Menegatti *et al.* 1998; Luciani *et al.* 2001; Weissert & Erba 2004) or shallow platform sections (e.g. Strasser *et al.* 2001; Wissler *et al.* 2003) in the northern Tethys, the general trend of our data is similar. The absolute values fit well to measurements from the southern Tethys (e.g. Oman: Immenhauser *et al.* 2005; Tunisia: Heldt *et al.* 2008) or the Pacific (Jenkyns & Wilson 1999; Price 2003).

Menegatti *et al.* (1998) divided the Cismon carbon isotope stratigraphy curve for the Upper Barremian and the Aptian in eight segments (C1–C8), widely used for subdividing Barremian–Aptian carbon isotope curves (e.g. de Gea *et al.* 2003;

(a) Section A, Gebel Raghawi, Late Barremian-lower Upper Aptian

Section D, Gebel Rizan Aneiza Upper Aptian

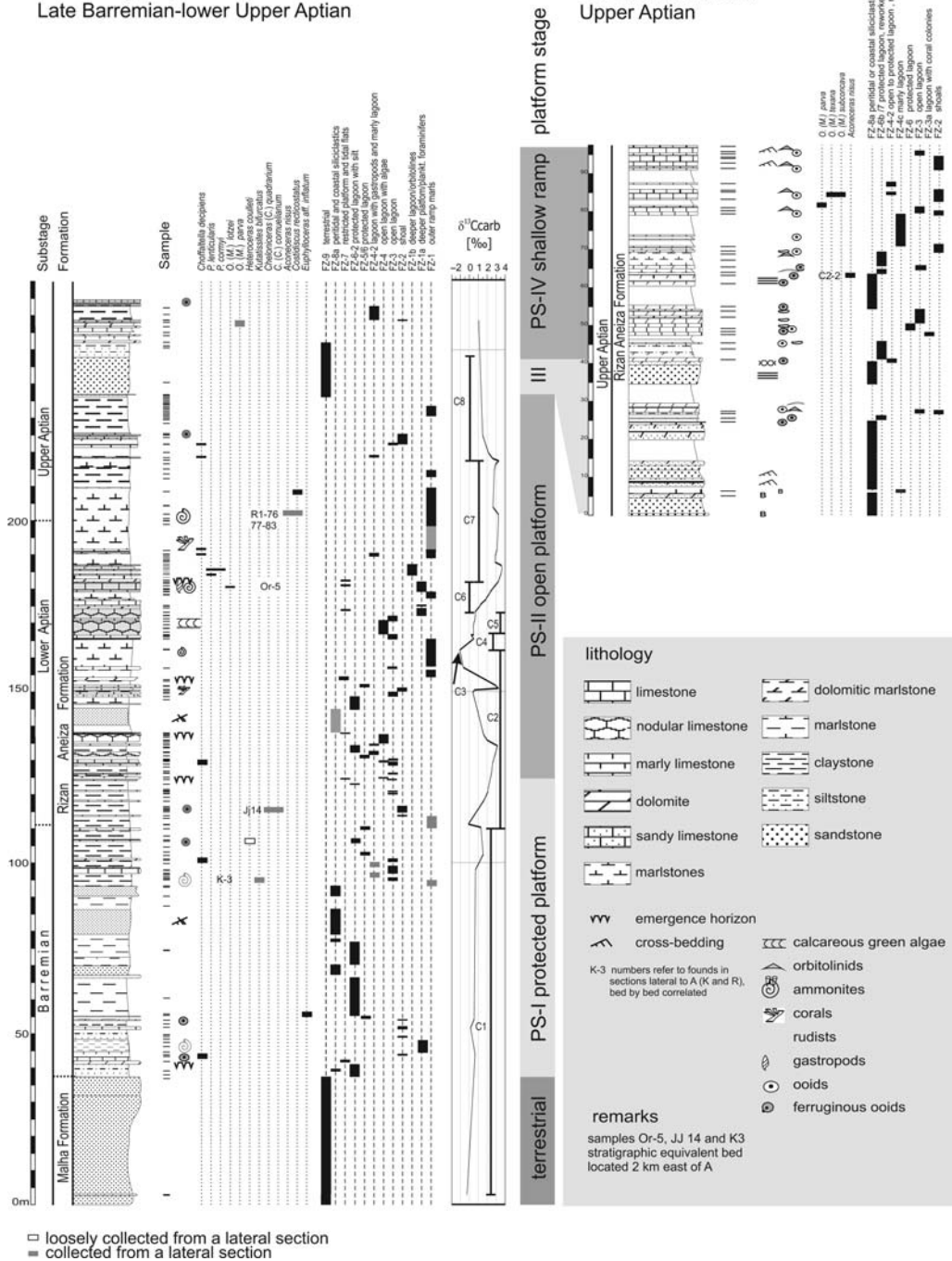


Fig. 3. Sections A (Gebel Raghawi), D (Rizan Aneiza), and GA (Gebel Amrar) reflect a transect across the Upper Barremian–Lower Aptian shallow shelf in North Sinai. The sections include lithology, $\delta^{13}\text{C}$ isotope bulk rock values, the occurrence of biostratigraphic marker fossils, and the facies interpretation.

(b) Section GA,
Gebel Amrar
Late Barremian-lower Upper Aptian

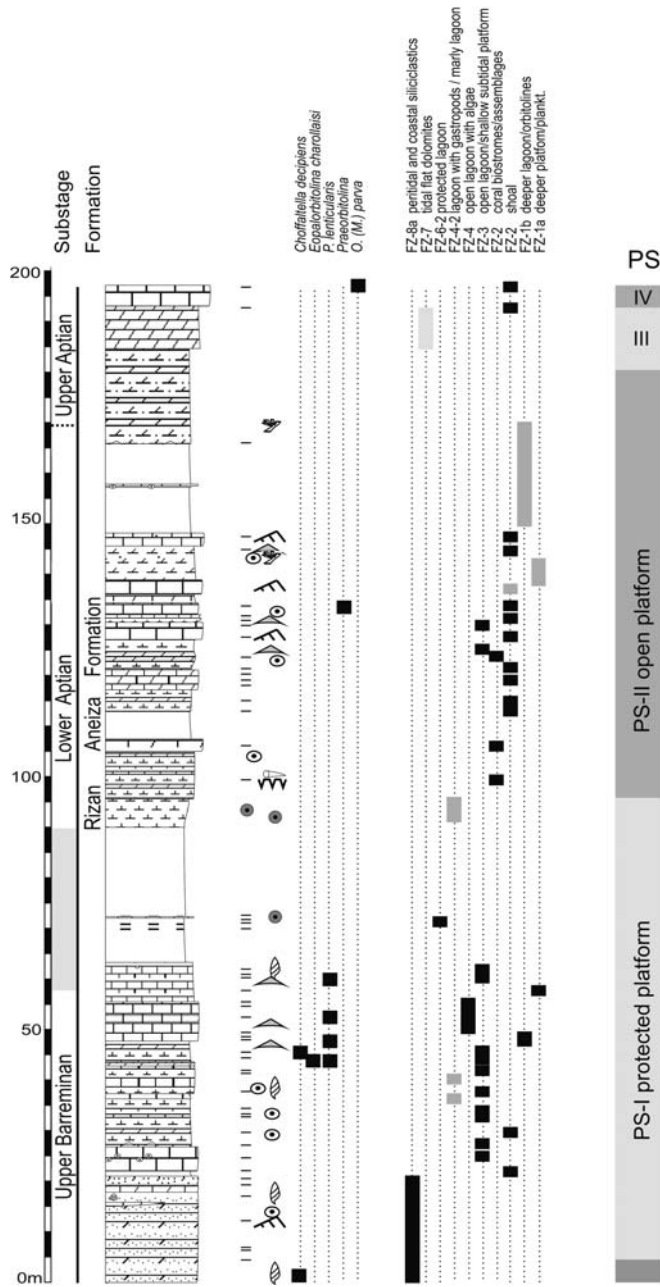


Fig. 3. (Continued)

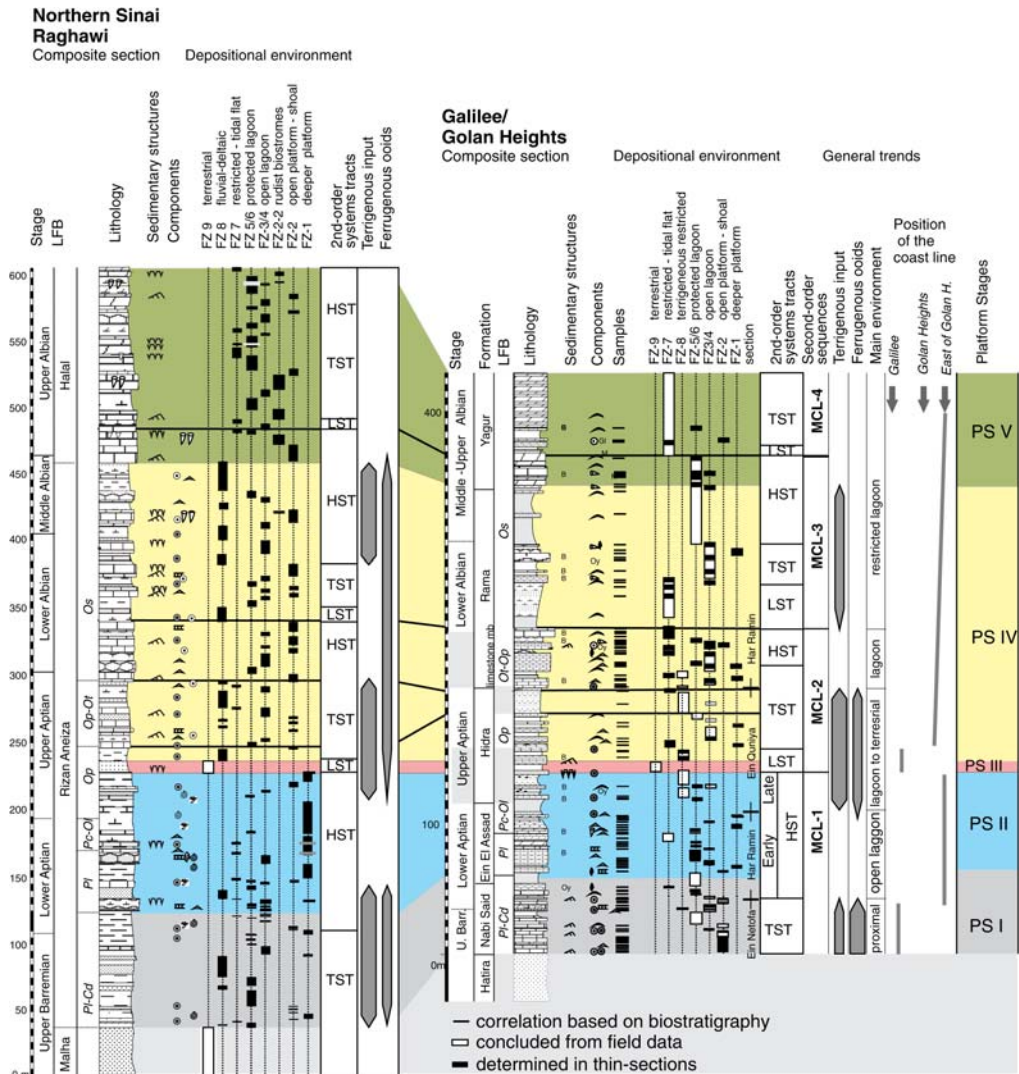


Fig. 4. Correlation of the North Sinai and Galilee–Golan Heights succession. A North Sinai standard section and the Raghawi standard section was chosen, for Galilee–Golan Heights a composite section was drawn from the sections Har Ramin and Ein Quniya. Indicated are the biostratigraphic interpretation (based on the LFBs), the depositional environment, the interpretation of the second-order sequences, the main changes in detrital input, and ferruginous ooid content, as well as for the Galilee–Golan Heights area the main environmental interpretation and the position of the palaeocoastline.

Heimhofer *et al.* 2004; Immenhauser *et al.* 2005; Renard *et al.* 2005; Heldt *et al.* 2008). The segments are dated by planktic foraminifera and calcareous nanoplankton zones (Menegatti *et al.* 1998; de Gea *et al.* 2003; Föllmi *et al.* 2006). The sections studied can be correlated with the segments as follows: the Upper Barremian interval, characterized by bulk carbon isotope values between -0.5‰ and 3.0‰ , may correlate with segments C1 and C2. The strong decrease to values, around -0.1‰ , and

a subsequent increase to 1.0‰ , reflect the intervals C3–C4. A relative stable segment may correlate with C5, widely interpreted as reflecting the Oceanic Anoxic Event (OAE) 1a (Menegatti *et al.* 1998; Luciani *et al.* 2006). The following increasing carbon isotope values in Cismon (C6) are reflected by an increase to a value around 3.5‰ . C7 is indicated again by stable carbon isotope values. The subsequent strong decrease in carbon isotope values reflects the change from segment C7 to C8.

The Barremian/Aptian boundary in North Sinai coincides with a negative carbon isotope peak between C1 and C2 at 115 m (Raghawi section A, Fig. 3a), which correlates with an interval around the Barremian/Aptian boundary of Moullade *et al.* (1998) and Godet *et al.* (2006). Föllmi *et al.* (2006) interpreted this peak as marking the Barremian/Aptian boundary. The equivalent of an OAE 1a is located at 160 to 175 m in the Raghawi section, which is in the Middle *L. cabri/deshayesi* zone according to Ogg (2004). The Lower/Upper Aptian boundary is suggested in a position just below the C7–C8 interval boundary around 200 m in the same section (Fig. 3a).

Stratigraphical interpretation and correlation of the sections

All data on stratigraphy are summarized in the regional correlation for the southern Levant Platform (Fig. 4). The first marine sediments are dated as Late Barremian by *Kutatissites bifurcatus* and *Heteroceras couletti* at the lower part of Raghawi sections A, K and R in North Sinai and by *Eopalorbitolina charollaizi* in the Amrar section (GA, North Sinai) and Ein Netofa section (Galilee). The occurrence of *P. lenticularis* and *C. decipiens* in all sections indicate LFB *Pl–Cd*. The Barremian/Aptian boundary is characterized by the FO of the Lower Aptian index species *Triploporella marsicana* (Masse 1998) in Galilee/Golan Heights and is correlated with an interval above the last occurrence of *H. couletti* and *K. bifurcatus* in North Sinai. The boundary is possibly located at the negative carbon isotope peak at 115 m (Raghawi section A). This interpretation coincides widely with that of Abu-Zied (2007), based on small benthic and planktic foraminifers for the Raghawi area.

The occurrence of *P. lenticularis*, *C. decipiens*, *P. cormyi*, *P. wienandsi* and *O. (M.) lotzei* allows the subdivision of the Lower Aptian into the LFBs *Pl* and *Pc–Ol* in both areas (Figs 3 & 4). While LFB *Pl* comprises the basal Lower Aptian, LFB *Pc–Ol* widely coincides with the negative isotope interval marking the OAE 1a in the upper Lower Aptian.

In North Sinai, the Lower/Upper Aptian boundary is indicated by the FO of *A. nesus* [*C. (E.) subnodosocostatum* ammonite zone] and a decrease of $\delta^{13}\text{C}$ values (Raghawi, section A, Fig. 3). This is 35 m below the boundary defined by Abu-Zied (2007) on the base of planktic foraminifers and suggested by Morsi (2006) on the base of ostracods. The upper part of the basal Upper Aptian *C. (E.) subnodosocostatum* ammonite zone furthermore comprises the FO of *O. (M.) parva* (e.g. Rizan Aneiza sections D and RN) and *C. (E.) tschernyschewi* (Fig. 3). In the Raghawi area, LFB *Op–Ot* is indicated

only a few metres above the FO of *O. (M.) parva* (Fig. 3) indicating a late FO of *O. (M.) parva* in comparison to other studies (Lower/Upper Aptian boundary according to Arnaud-Vanneau 1998).

In Galilee/Golan Heights, the Lower/Upper Aptian boundary is suggested to be 40 m below the FO of *O. (M.) parva*, according sequence stratigraphical and lithological correlations with North Sinai.

The correlation of the Upper Aptian–Albian succession between both areas is more difficult because of the rare biostratigraphical markers in the Galilee–Golan Heights region, while the North Sinai succession is quite well dated. The Aptian/Albian boundary in North Sinai is marked by two distinct ostracod assemblages and confirmed by graphic correlation (Bachmann *et al.* 2003). This boundary was interpreted to be within the Limestone Member (lower Rama formation) in the Golan Heights (Bachmann & Hirsch 2006). Based on the correlation of second-order sequences between Sinai and the Golan Heights (presented in this paper, Fig. 4) the boundary is expected to be located lower in the section, around the boundary Hydra/Rama Formation, which is conformed to ostracod data from Rosenfeld *et al.* (1995). In North Sinai, the Early/Middle Albian boundary is placed above the FO of *Eoradiolites liratus* (occurring since the latest Early Albian, Steuber & Bachmann 2002), by graphic correlation and the FO of *Desmoceras (D.) latidorsatum* (Bachmann *et al.* 2003), which first appears in the Late Albian (Gale *et al.* 1996). The Middle/Late Albian boundary is characterized by the LO of *O. (M.) parva* and the FO of *N. simplex* (Bachmann *et al.* 2003). Biostratigraphical data on the upper part of the succession in Golan–Galilee are generally rare and is based on ostracod assemblages or rare findings of the ammonite *Knemicerias* in Galilee (Rosenberg 1960; Rosenfeld *et al.* 1995).

Platform development

Facies zones: platform environments

The classification of facies zones (FZs) and the interpretation of the depositional environments are summarized in Figure 5, following the classification given by Bachmann & Hirsch (2006, Galilee–Golan Heights) and Bachmann & Kuss (1998, Sinai). The FZs range from deeper open platform to terrestrial and siliciclastic-influenced restricted platform. Nearly every FZ contains more than one facies type reflecting similar environments of deposition. Facies interpretations involve the comparison with other Barremian–Albian Tethyan platforms (Arnaud-Vanneau & Arnaud 1990; Masse 1993; Masse *et al.* 1995; Husinec 2001; Bernaus

	Name	Microfacies	Diagnostic-Components	Subordinate components	Sedimentary structures	Depositional environment / energy conditions	Occurrence
Deeper platform	FZ-1	MFT 1: marls with planktic foraminifers and ammonites	planktic foraminifers (mainly hedbergellids), and/or ammonites (often pyritic), radiolarians	small solitary and colonial corals, typically at the base of a marly unit, benthic foraminifers (textulariids, <i>Choffatella</i> , <i>Lenticulina</i>), echinoids, echinoderm debris, shells and intraclasts	thick marlstone beds	deeper inner to outer platform / ramp low-energy, below wave-base	Sinai: Rizan Aneiza Fm.
		MFT-1b: bioclastic to intraclastic wackestones to packstones, MFT-1a: often rich in orbitolinids orbitolinid marlstones	Divers bioclasts, discoidal orbitolinids (<i>Palorbitolina</i> , <i>Praeorbitolina</i> , <i>Orbitolina</i> (M)), intraclasts, smaller and larger benthic foraminifers (textulariids, miliolids, <i>C. decipiens</i> , <i>Lenticulina</i> , complex litiolids, <i>Buccicrenata</i>), frequently planktic foraminifers groundmass: micritic	often abundant echinoderms, sponge spicules, calcareous red algae (<i>Permoalcalulus</i>), calcareous green algae, mud peloids and cortoids, +/- gastropods, rudist debris, ostracods	thin bedded or nodular-bedded marlstone – limestone alternation or limestone couplets components poorly sorted, often poorly washed	partly bottom currents, rich in nutrients (*)	Sinai: Lower Rizan Aneiza Fm. Galilee/Golan: Top Ein El Assad Fm., Rama Fm.
High-energy platform	FZ-2	MFT 2a:oolithic grainstones, MFT 2b: oolithic–bioclastic grainstones, MFT 2c: bioclastic grainstones MFT 2d: few packstones, all partly with quartz and/or ferruginous ooids MFT 2e: intraclastic grainstone	ooids, bioclasts, intraclasts, bivalves, echinoderm debris, cortoids, coated grains 2d partly ferruginous ooids, quartz grains and less divers biota groundmass: sparitic	bryozoans, rare and diverse benthic foraminifers (orbitolinids, cuneolinids, complex Lituolaceans, <i>Buccicrenata hedbergii</i> , <i>Choffatella decipiens</i> , <i>Charentia cuvillieri</i>), dasycladaceans, udoteaceans, red algae (e.g. <i>Marinella</i>), rudist debris, gastropods	cross-bedding, channels, up to 15-m-thick limestone couplets	shallow outer platform / high-energy shoals	Sinai: entire succession Galilee/Golan: Nabi Said Fm. dominated by MFT 2a Ein El Assad Fm.: rare
Rudist biostromes	FZ-2-2	MFT 2-2a:rudist boundstones packstone with rudist or rudist debris MFT 2-2b: packstone with incrusting organisms	rudist, rudist-debris, shells, bioclasts, benthic foraminifers (orbitolinids, miliolids) groundmass: micritic +/- incrusting organisms (red algae, cyanophyceae, <i>Lithocodium/Baccinella</i>),	benthic foraminifers (complex litiolaceans), dasycladaceans, udoteaceans, echinoderm debris, gastropods, mud peloids, cortoids, rare ooids	up to m-thick or massive beds, lentiform, lateral extension m to km.	shallow outer platform/ low energy	Sinai: Rizan Aneiza Fm.: small biostromes (10s of meters wide) Halal Fm: large extended biostromes Galilee: Albian, Mount Carmel, large extended biostromes/bioherms (Sass & Bein 1982)
Coral biostromes	FZ-2-3	packstone to boundstone with coral colonies	corals colonial, red algae, echinoids groundmass: sparitic, micritic, often dolomitized	+/- incrusting organisms (cyanophyceae), green algae	small ellipsoidal lenses intercalated in marlstones or well bedded couplets up to 4 m thick	shallow subtidal low-energy	Sinai Rizan Aneiza Fm.

Fig. 5. Facies classification and interpretation on the base of components, composition and sedimentary structures.

	Name	Microfacies	Diagnostic-Components	Subordinated components	Sedimentary structures	Depositional environment / energy conditions	Occurrence
Open platform - shallow-subtidal	FZ-3	MFT 3: bioclastic to intraclastic packstones and wackestones with diverse bioclasts MFT-3a: oncoid ps	diverse bioclasts and/or intraclasts, echinoderm debris, bivalves (shells), dasycladaceans, udoteaceans, mud peloids +/- oncoids and cortoids groundmass: micritic or partly poorly washed	common gastropods, rare diverse benthic foraminifers (cuneolinids, textulariids, miliolids, larger agglutinated foraminifers, <i>B. hedbergii</i> , <i>C. decipiens</i> , <i>Praechrysalidina</i> , <i>C. cuvillieri</i>), oysters, rudists, sponge spicules	well-bedded, poorly sorted and common bioturbated sediments	open platform shallow subtidal / low-energy	Sinai: entire succession Golan/Galilee: Nabi Said Fm with cortoids, Ein El Assad Fm typically highly diverse, with calcareous algae
		MFT-3c: orbitolinid-intraclastic packstones MFT 3e: bioclastic-intraclastic packstones	dominately: orbitolinids and intraclasts components less divers: only bioclasts, intraclasts, echinoderms and shells abundant, all others are common to rare	orbitolinids, calcareous algae (chyanophyceans), coral debris, benthic foraminifers (textulariids, miliolids, complex Lituolaceans) Golan: often rich in rudist debris and poor in calcareous algae			Sinai: entire succession Sinai: Rizan Aneiza Fm Golan: Limestone Mb., Rama Fm
	FZ-3-2	MFT 3-2 bioclastic packstone with quartz and/or ferruginous ooids	additionally quartz and ferruginous ooids			3b shallow subtidal influence by siliciclastic input	Sinai: Rizan Aneiza Fm Nabi Said Fm, Hidra Fm, lower Unit 0, Unit A
open lagoon	FZ-4	MFT 4: bioclastic packstones and wackestones rich in calcareous green algae	calcareous green algae (dasycladaceans and udoteaceans: <i>Cylindroporella</i> , <i>Pseudoactinoporella</i> , <i>Neomeris</i> , <i>H. dinarica</i> , <i>Acicularia</i>), abundant and diverse foraminifers (miliolids, textulariids, cuneolinids, larger agglutinated foraminifers s. FZ-3)	gastropods, echinoderm debris, bivalves, rare sponge spicules and ostracods, few <i>Pormocalculus</i>	well-bedded or nodular bedded, poorly sorted and common bioturbated	open platform shallow subtidal characterized by calcareous algae	Sinai: Rizan Aneiza Fm Galilee/Golan: Lower Aptian only; Ein El Assad Fm , Nabi Said Fm: rare
		MFT 4b: bioclastic packstone with gastropods	large gastropods, shells, abundant echinoderm debris, bioclasts and intraclasts +/- ferruginous ooids	benthic foraminifers (miliolids, textulariids), oncoids, cortoids, locally enriched in rudist fragments, dasycladaceans, locally iron ooids partly with ammonites and belemnites	nodular to planar bedded locally bioturbated	open to protected shallow subtidal, with ferruginous ooids closely related to the coast	Sinai: Rizan Aneiza Fm with ammonites/Bellemnites only middle PS II
open to protected lagoon - shallow subtidal	FZ-4-2	MFT 4c: marlstones with gastropods, and shells marlstones with orbitolinids marlstone with silt marlstone with few bioclasts	gastropods, shells, ostracods +/- orbitolinids	locally abundant iron ooids, echinoderms, small solitary and colonial corals		protected platform to marly lagoon, subtidal	Sinai: entire succession
		MFT 4d: intraclastic packstone with reworked components	intraclasts, reworked cyanophyceans or reworked benthic foraminifers (textulariids, miliolids and cuneolinids), +/- ferruginous ooids	bioclasts, orbitolinids, echinoderm debris benthic foraminifers	often laminated	protected to restricted platform, reworked	Sinai: Lower Rizan Aneiza Fm

Fig. 5. (Continued)

	Name	Microfacies	Diagnostic-Components	Subordinated components	Sedimentary structures	Depositional environment / energy conditions	Occurrence
protected lagoon	FZ-5	wackestones to mudstones, rarely packstones with <i>H. dinarica</i>	calcareous green algae (mostly <i>H. dinarica</i>), shells, echinoderm debris	Common benthic foraminifers (mostly cuneolinids, less abundant miliolinids, orbitolinids, textulariids), calcareous debris, ostracods and sponge spicules, mud peloids	nodular- or planar-bedded, poorly sorted and common bioturbated sediments	protected platform open lagoon characterised by <i>H. dinarica</i>	Sinai: Lower Rizan Aneiza Fm Galilee/Golan: Nabi Said Fm: Top only, Ein El Assad Fm, Rama Fm: rare
	FZ-6	mudstones to wackestones, rarely packstones with foraminifers and wackestones to floatstones with rudists	benthic foraminifers (diverse miliolids, textulariids and cuneolinids) rudists	shells, echinoderm debris, sponge spicules, gastropods, <i>H. dinarica</i> , <i>Acicularia</i> , ostracods, mud peloids rudists (in situ or as large rudist debris)	lamination or nodular bedding, occasionally, mud cracks	protected platform lagoon	Sinai: Upper Rizan Aneiza Fm Galilee/Golan: Nabi Said, Ein El Assad, Rama Yagur Fms. wackestones to floatstones with rudists occur mainly in the Upper Aptian–Albian
	Fz-6b	intraclastic packstones and wackestones with few bioclasts	intraclasts, calcareous green algae, cyanophyceans, shells, echinoderm debris	benthic foraminifers (miliolids, textulariids, orbitolinids), gastropods, echinoderm debris	thin beds within marlstones	protected lagoon, reworked	
	FZ-6-2	marlstones, silty marlstone	ostracods, silt, peloids, gastropods	benthic foraminifers, bioclasts, coral fragments,	non-bedded marlstones, partly bioturbated	marly lagoon	Sinai: Lower Rizan Aneiza Fm.
Restricted platform	FZ-7	MFT 7: mudstones and wackestones, rarely packstones often characterised by microbial laminae, birdseyes or mudcracks pure dolomites	microbial mats, ostracods, or gastropods, spicules (monaxons of siliceous sponges) partly rich in small intraclasts and mud-peloids	calcareous debris, few foraminifers (Miliolids), mud peloids, shells occasional ferruginous ooids or quartz silt, benthic foraminifers and +/- orbitolinids, shell fragments and echinoderm debris	lamination, mudcracks, birdseyes or reworking	restricted platform and tidal flats occasional reworked and emerged	Sinai: Lower Rizan Aneiza Fm. Upper Rizan Aneiza Fm. at sequence boundaries Galilee/Golan: Ein El Assad Fm., Rama Fm., Yagur Fm.
	Platform with siliciclastic influence	FZ-8	MFT 8: laminated, cross-bedded or bioturbated sandstones, claystones, marlstones, sandy mudstone and wackestones or dolomites	quartz and/or ferruginous ooids	few bivalves, oysters, echinoderm debris, gastropods, ostracods, bioclasts, plant remains iron crust at the top of some beds	lamination or cross-bedding, bioturbation	protected to restricted platform with high siliciclastic input, fluvial or deltaic influence
MFT 8a: laminated, crossbedded partly bioturbated sandstones and siltstones, subordinated claystones and marlstones			quartz, reworked intraclasts, dolomitic cements	often abundant plat remains, rarely few bivalves and bioclasts +/- ferruginous ooids	lamination or cross bedding	platform closely related to the coastline, often peritidal influence	Sinai: Rizan Aneiza Fm.
Terrestrial	FZ-9	cross-bedded sandstones	quartz, ferruginous crusts	kaolinite	trough cross bedding, , unsorted	siliciclastic supratidal to fluvial environment	Sinai: Lower Rizan Aneiza Fm. Galilee/Golan: Hidra Fm.

Fig. 5. (Continued)

et al. 2003; Masse *et al.* 2003), and particularly with those in the southern Tethys (Pittet *et al.* 2002; Van Buchem *et al.* 2002; Immenhauser *et al.* 2005).

Most FZs occur in both study areas and at different stratigraphical levels. Their distribution is indicated for three Upper Barremian–Aptian sections: section A (Fig. 6e & f) (supplemented by data from the sections K and R), sections GA and D (Figs 1c, 3a, b & 6d). To investigate the lateral facies variations in North Sinai during the Upper Aptian–Lower Albian (Fig. 7) sections D and MgE are added to data by Bachmann & Kuss (1998) and Bachmann *et al.* (2003). For the Galilee–Golan Heights the facies description summarizes data presented in Bachmann & Hirsch (2006).

Two standard sections illustrate the facies variations between the platform settings at Sinai and Galilee–Golan Heights (Fig. 4). General trends for terrigenous input, formation of ferruginous ooids, main carbonatic components, and grain diversity are added. Lateral variations of FZs are recognized when correlating the different sections and allow an interpretation of the platform geometry for both areas studied during several time slices. Vertical variations indicate the changes of the platform environment associated with varying external and internal parameters (e.g. climate, sea-level change, sediment accumulation).

The distribution of FZs characterizes major lithological, facies, and environment changes, leading to a subdivision of five PS (PS I to V) within the evolution of the Levant Platform. These PS are decoupled from the definition of formations. Facies development is described separately for both study areas, to focus on the regional geometric patterns.

The North Sinai platform stages

PS I. PS I comprises the first Lower Cretaceous marine sediments and is characterized by limestones, marlstones, and siliciclastics deposited in varying depositional environments reaching from terrestrial to deeper marine.

PS I comprises the lowermost Rizan Aneiza Formation (Upper Barremian–basal Lower Aptian, LBFs *Pl–Cd*, and lower *Pl*).

An alternation of marl, siltstone, dolomite, and limestone belonging to various FZs (FZ 1 to 8, Fig. 5) in the northern sections A (Raghawi, 85 m thickness) and GA (Amrar, 95 m thickness, Figs 3 & 7) is interfingering with terrestrial sandstones (Malha Formation, FZ 9) 5 km south of Raghawi (Mansoura area – Fig. 1c).

At section A (Figs 1c & 3a) PS I is dominated by protected lagoonal environments, characterized by bioclastic wacke and packstones, with benthic foraminifers, shell and echinoderm debris and

oncooids (FZ 6), partly rich in orbitolinids and cyanophyceans. These limestones alternate with marlstones, silty marlstones, and siltstones containing few autochthonous benthic foraminifers, ostracods, small solitary coral colonies, echinoderm debris, and further bioclasts (FZ 6-2) that are indicating a varying terrestrial input. Several levels contain ferruginous ooids. In the lower part, intercalated peritidal to coastal sandstones and siltstones (FZ 8a) indicate two regressive events. In the same interval, ammonite-bearing marlstones indicate a sporadic influence of open-marine conditions. Among those ammonites are several phylloceratids (e.g. *Euphyloceras aff. inflatum*), which are interpreted as reflecting deeper-marine conditions (Westermann 1996). Intercalations of oolitic, intraclastic and bioclastic grainstones (FZ 2) mark the repeated influence of shallow subtidal, high-energy conditions. Upward increasing, intercalated limestones rich in oncooids (FZ 3, mainly MFT 3a) reflect increasing open platform shallow subtidal conditions. In the uppermost part of PS I frequent intercalated dolomites (early diagenetic dolomite formation), are suggested as representing short events of emergence. The upper boundary of PS I is settled at the point of increasing carbonate content and marked by the last occurrence of the ferruginous ooids and the first occurrence of dasycladacean-rich open lagoons (FZ 4) above.

At section GA (Figs 1c & 3a) the succession is dominated by oncooid-rich limestones of FZ 3, showing a trend to more open lagoonal/platform conditions. Siliciclastic input is less frequent and of finer grain size, while ferruginous ooids occur only rarely. Deeper platform environments (FZ 1), comparable to the ammonite bearing beds at section A, occur only in the upper part of PS I at section GA.

About 5 km towards the south, terrestrial sediments characterize PS I and indicate that the coastline was located north of the Gebel Mansour (Fig. 8a, f). The proximal position of section A is reflected by intercalated coastal sediments and high contents of clay and ferruginous ooids. Further north, at the distal section GA, the open-marine facies lacks coastal influence. However, depositional environments are partly shallower than in the proximal SW, suggesting deposition on a submarine high, separating the protected area at section A from open-marine environment. The open-marine deeper environments are expected to be in a close position to the study area because of the occurrence of phylloceratids.

PS II. During PS II open platform environments in the north are interfingering with terrestrial sediments in the south.

The main part of the Lower Aptian sediments and the first metres of the lowermost Upper Aptian (lower LFB *Op*-zone/lower *C. (E.) subnodocostatum* zone), belong to PS II.

Marine limestones, marlstones, siltstones, and sandstones of PS II crop out at section GA (90 m thickness, Fig. 3b) and at section A (110 m thickness, Figs 3a & 6e, f), while at Gebel Mansour further to the south, only terrestrial siliciclastics occur. PS II starts with shallow-subtidal open-marine environments containing diverse bioclasts and dasycladaceans (section A, FZs 3 and 4). Intercalated near-shore sandstones (FZ 8) and a remarkable red-brownish dolomite horizon (early diagenetic dolomite formation, Fig. 6e) are suggested as representing events of regression and emergence. Above, marlstones containing some ammonites (FZ 1) are overlain by limestones rich in calcareous algae (FZ 4), limestones with diverse biota and planktic foraminifers (FZ 1a) and limestones characterized by high amounts of orbitolinids (FZ 1b). About 40 m of marlstones with corals at the base and ammonites and planktic foraminifers (FZ 1) are marked by upward decreasing carbonate content. About 4 m of intercalated grainstones with ferruginous ooids (FZ 2), indicate a short event of shoaling. Maximal 10 m of marly claystones of FZ 1 form the top of this interval. The upper boundary of PS II is formed by an erosional unconformity, which cuts into the upper marly claystone at section A and into the ferruginous-ooid interval below E of the section A. At Gebel Amrar limestones deposited in high-energy shoal environments dominate the lower part of PS II, while silty marls of open-marine and lagoonal environments (FZ 1 and 6-2) occur in the upper part.

Generally PS II is characterized by subtidal open-platform environments with upward increasing influence of open-marine conditions. The coarse grained terrestrial input is strongly reduced in the upper part and ferruginous ooids are missing until a short shoaling interval, allowing the deposition of near coast sediments with ferruginous ooids, at Gebel Raghawi.

Its southward proximal regional extension is very similar to PS I. Terrestrial sediments crop out in the entire southern region and indicate a widely unchanged position of the coastline between the northern Raghawi and Mansour area (Fig. 1). The only exception is one marly bed with corals, which was observed in a single locality at southern Gebel Maghara close to section A (Fig. 7). Because of the erosive nature of PS III above, a now eroded uppermost part of PS II, ranging further to the south, cannot be excluded. The deposition of high-energy shoals at section GA with deeper sediments behind makes the existence of a barrier in that area highly probable.

PS III. Sandstones deposited in terrestrial and coastal environments characterize PS III.

This interval is attributed to the lowermost Upper Aptian (*subnodocostatum* zone; Fig. 2).

At section A (most proximal section) the interval consists of only 10 m of caolinitic quartzose sandstones (Fig. 6e), which are interpreted as terrestrial deposits (FZ 9). The erosional base of the succession cuts into different levels of the underlying succession. At section D (Fig. 1c) 40 m of coastal siliciclastic sediments (FZ 8a) mark that interval, which are two times interrupted by lagoonal and shoal originated carbonates (FZ 4 and 2). At section GA the interval is formed of 10 m of tidal flat dolomites (Fig. 3b).

Compared to PS I and II, the coastline moved to the north and was now located between sections A and GA, close to sections RN and D (Fig. 1). Section A comprises the terrestrial realm, while sections RN and D indicate a near shore position. The more distal section GA was also partly emerged, but not affected by siliciclastic deposition, speaking for a local high/swell (Figs 7 & 8a).

PS IV. Shallow subtidal marine limestones, deltaic siliciclastics, and a southward transgression mark this platform stage.

PS IV comprises the upper Rizan Aneiza Formation, which was deposited during the Late Aptian until the end of the Middle Albian (Bachmann *et al.* 2003).

Marine sediments of this interval were documented from sections D (Fig. 3a) and RN (240 m, Fig. 7), section R (225 m, Fig. 4), sections ME and M (190 m, Figs 7 & 6h), and section MgE (140 m, Fig. 7). In the northern and central distal sections, the marine sedimentation starts in the upper *C. (E.) subnodocostatum* zone (sections C, RN and R), while in the proximal southeastern area the first marine sediments are dated as Lower Albian (sections M, ME; Bachmann *et al.* 2003; and section MgE, Fig. 7). At the northern section RN marlstone–limestone alternations of the shallow-subtidal FZ 3 to protected lagoon FZ 6 with some intercalated small-scaled rudist biostromes (FZ 2-2), bioclastic to oolitic shoals (FZ 2), and some meters of open-marine sediments (FZ 1) prevail. The Raghawi–Mansour area was characterized by a delta system with sandstones, siltstones, and marlstones of FZ 8, prograding repeatedly into the area studied and alternating with shallow subtidal, open-marine (FZ 3), and lagoonal sediments (FZs 4, 6 and 7; Bachmann & Kuss, 1998) and furthermore high energy shoals (FZ 2, Fig. 5). The amount and frequency of fine and coarse grained siliciclastic intercalations increase to the SE until they dominate the succession at section MgE (Fig. 7). Up to 4 m thick rudist biostromes (FZ 2-2) with

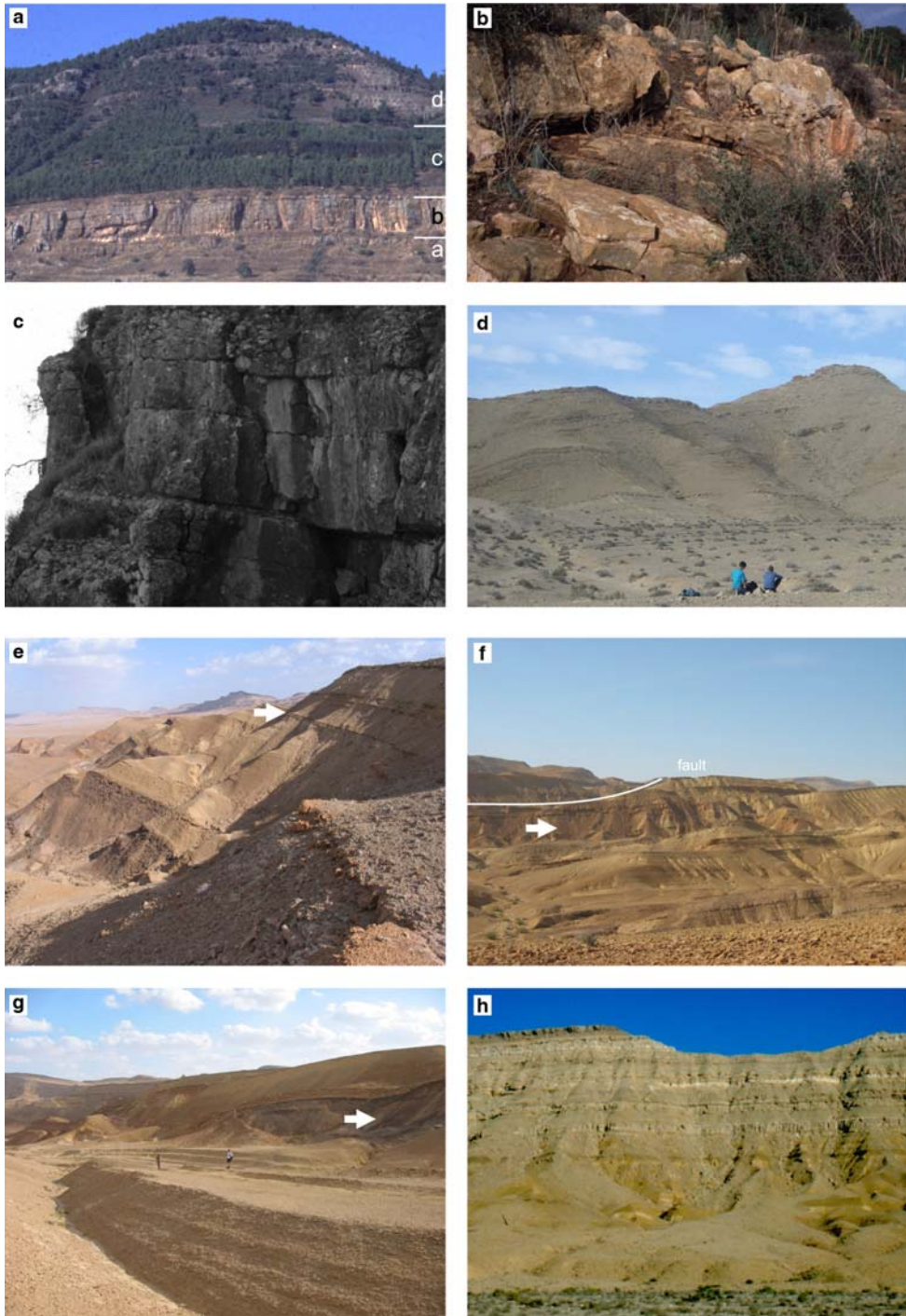


Fig. 6. Facies and bedding-patterns of the Upper Barremian–Albian strata. (a) Nabi Said Fm. The Har Ramin section, Galilee, comprises the entire Lower Aptian–Middle Albian succession. (b) Ein El Assad Fm. In the Ein Netofa section (Galilee), the cross-bedded limestones of the Upper Barremian Nabi Said Formation are well developed. (c) Hidra Fm. Well-bedded limestones mark the Ein El Assad Formation in the Har Ramin section. (d) Rama Fm. The Rizan Aneiza

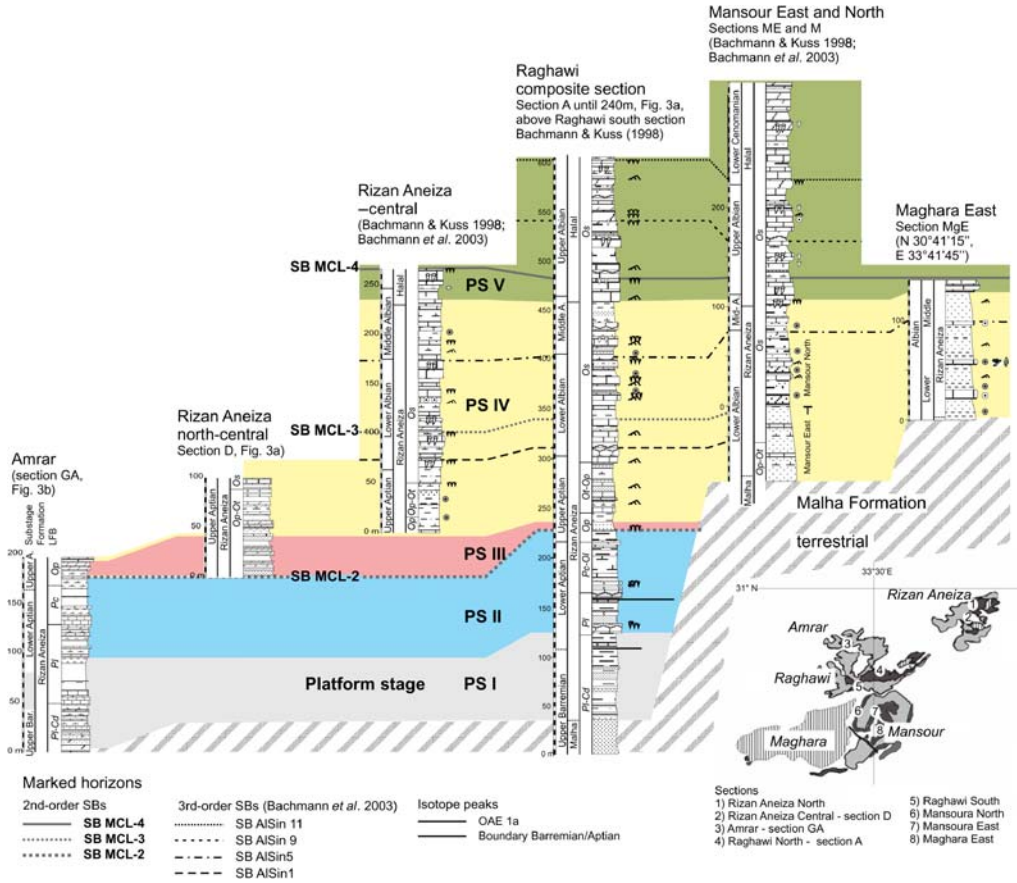


Fig. 7. Correlation of the sections in North Sinai summarizing new and known sections (Bachmann *et al.* 2003). The sections are correlated along marker horizons, sequence boundaries, and the biostratigraphic frame. Platform stages are indicated by different colours. The location of the sections is shown on the small map.

lateral extensions of tens of metres are intercalated in the succession at sections RN, D, A and ME (Figs 7 & 6h). At section A, an up to 4 m-thick coral biostrome (FZ 2-2a) is intercalated in the lower part of PS IV, while the entire succession is marked by high amounts of ferruginous ooids, which decrease in frequency and amounts distally (section RN, Fig. 7). Intercalated emergence

horizons are common and marked by rhizolites or ferruginous crusts that can be correlated over large areas in the region (Bachmann & Kuss 1998). The facies evolution of PS IV reflects third-order sea-level changes (Bachmann & Kuss 1998).

All the described sections of PS IV follow a proximal–distal transect across the shallow shelf (Fig. 8). A retrogradation of facies belts and

Fig. 6. (Continued) Formation at its type-locality is characterized by marly and sandy limestones (section D). (e) Lower part of the Raghawi Section A: coastal sandstones marlstones, and upward increasing dolomites and limestone mark the Upper Barremian and Lower Aptian platform stages PS I and PS II (Rizan Aneiza Formation, Gebel Raghawi). The arrow indicates a prominent dolomitic horizon 150 m above the base of the section, which is interpreted as emergence surface. (f) At northern Gebel Raghawi the entire Barremian–Middle Albian succession crops out and is bounded in its upper part by a major reverse fault. The arrow indicates the terrestrial sandstones of PS II shortly above the Lower–Upper Aptian boundary. The succession above the sandstone shows the Upper–Middle Albian PS IV marked by increasing limestone content (Upper Rizan Aneiza Fm). (g) The figure comprises nodular limestones, marlstone, and the sandstone (arrow) of the uppermost Lower Aptian to lowermost Upper Aptian. (h) The Upper Aptian to Lower Cenomanian succession at Gebel Mansoura is characterized by deltaic sediments in its lower part and pure limestones with huge rudist biostromes (arrow) in the upper part.

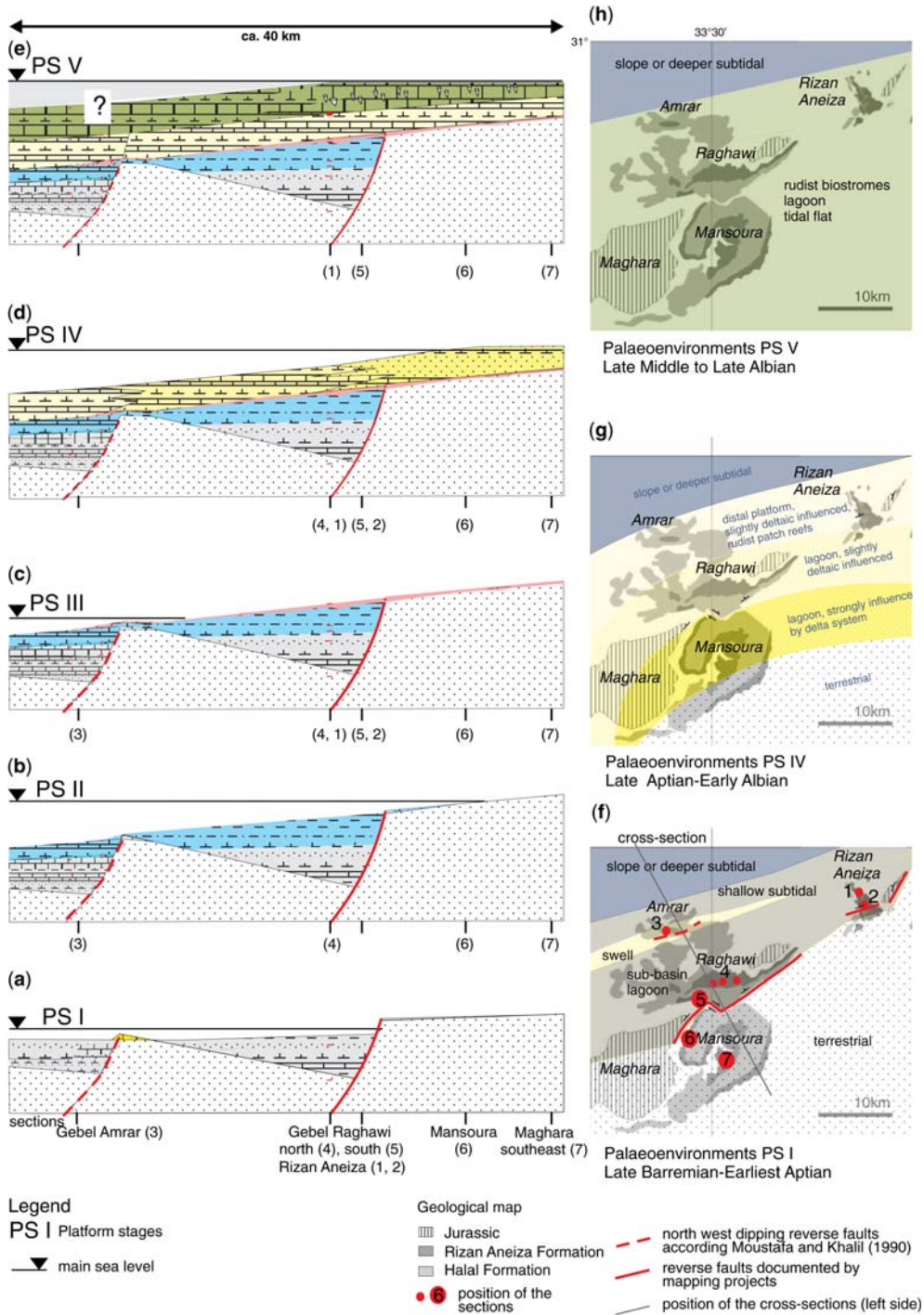


Fig. 8. Schematic transect through the North Sinai shallow shelf displays the Late Barremian–Aptian evolution and involves the factors extension along normal faults and sea level change (a–e). Palaeoenvironmental maps indicate the lateral extension of facies zones (f–h). (a, b) PS I and PS II are characterized by increasing sea level. (f) The southern coastline was located at the Raghawi–Mansoura normal fault, with a possible short-term southward transgression

transgression onto former terrestrial areas is obvious (Fig. 8). The coastline was located between Gebels Raghawi and Mansour during Late Aptian times, between Mansour and Maghara East around the Aptian/Albian boundary, south of Maghara area during Early and early Middle Albian times, and more than 50 km further south during the late Middle Albian (Bachmann & Kuss 1998). This step-wise retrogradation is also indicated by a southward decreasing thickness, which is mainly owing to a later onset of sedimentation (Fig. 8).

PS V. PS V is characterized by relatively uniform deposition of limestones in the entire region.

PS V comprises the lower part of the Halal Formation (Late Albian–Early Cenomanian, Bachmann *et al.* 2003). At Rizan Aneiza and Raghawi only the lower part of PS V crop out (section RN: 40 m, section R: 145 m, Fig. 4), but at Mansour (section M, Fig. 6h) and Maghara SE (section MgE) 200 m of sediment occur (Fig. 7).

The base of PS V is characterized by an up to 20 m thick rudist biostrome (FZ 2-2, sections RN, R, M, Figs 4 & 7), which is interfingering southward (section MgE) with lagoonal limestones (FZ 6a). In all localities, a sudden stop of the siliciclastic input occurs below this bed. Overlying this, limestone–marlstone alternations of FZs 5, 6 and 7 prevail. Marly lagoonal environments characterize PS V with high amounts of gastropods and orbitolinids (FZ 6-2) and the repeated formation of small and larger rudist biostromes (FZ 2-2) of protected lagoons, as well as stromatolithic tidal flats (FZ 7) above. Intercalated oolitic and bioclastic shoals (FZ 2) indicate high-energy facies. Open-marine subtidal facies are rare, while deeper platform facies types are missing. Repeated emergence horizons characterized by rhizolithes, tepee structures, dolomitic, and in the lowermost part by carstification are intercalated and reflect sequence boundaries of the third-order sequences (Bachmann & Kuss 1998). The increasing abundance of dolomitized tidal flat deposits (FZ 7) in the upper part of PS V indicates a general shoaling of the depositional area.

During PS V, the main position of the coastline was located clearly south of the investigated area (Bachmann & Kuss 1998). Decrease in siliciclastic input and short-termed sea-level lowstands produced emergence in contrast to the prograding delta wedges of former periods. Thickness of the

sediments is clearly higher in the respective distal sections. The lateral distribution of FZs indicates a very similar, shallow, protected marine environment covering large parts of the North Sinai platform (Fig. 7).

The Galilee–Golan Heights platform stages

The platform stages PS I–V are well documented at Galilee–Golan Heights and allow the correlation of four sections (Figs 1b & 9) with North Sinai. These sections represent a transect across the shallow shelf of the northeastern Levant platform located on both sides of the DST fault. The marine succession starts above terrestrial sandstones of the Hatira Formation.

PS I. In northern Israel/the Golan Heights PS I comprises the first marine Lower Cretaceous sediments similar to North Sinai. Limestones deposited in shallow subtidal environments predominate.

PS I correspond with the Nabi Said Formation, which is of Late Barremian to basal Early Aptian age (LBFs *Pl–Cd* and lower *Pl*) (Fig. 4).

In central Galilee, they are well exposed in the Ein Netofa section, but at the Golan Heights only a few metres of basal Lower Aptian occur (Bachmann & Hirsch 2006). The Ein Netofa section is characterized by about 32 m of cross-bedded oolitic and bioclastic grainstones, partly enriched in ferruginous ooids and quartz (FZ 2). They increasingly alternate upward with bioclastic packstones (FZ 3) and wackestones reflecting protected environments (FZ 4, 5 and 6). At the Golan Heights 10 m of sediment were deposited in protected lagoons with tidal flats (FZ 4 and 7).

During the Barremian, an open-platform high-energy facies belt (Ein Netofa section) was interfingering to the east and SE with terrestrial sediments (Hatira Formation) in the region between Galilee and Golan (Hirsch 1996). The abundance of ferruginous ooids and coarse grained quartz indicates the vicinity of the proximity to the coastal area, which retrograded during the Late Barremian–earliest Aptian to an area east of the Golan Heights. A slightly inclining ramp geometry is documented by a gradient from high- and low-energy open subtidal (FZ 2 and 3) facies occurring in the Ein Netofa section to protected subtidal environments (FZ 3 and 4) at Har Ramin, and intertidal facies-types (FZ 7) at the Golan Heights.

Fig. 8. (Continued) at the end of PS II. (c) A significant drop in sea level caused emergence of wide areas and erosion of the former relief. (d) During PS IV, a homoclinal ramp characterizes the depositional architecture. A delta system developed in the proximal areas, interfingering with lagoonal and shallow ramp sediments. (e) The strike of the facies belts changes from SW–NE to WSW–ENE. (f) During Late Albian down by rising sea-level, a shallow platform without major changes developed.

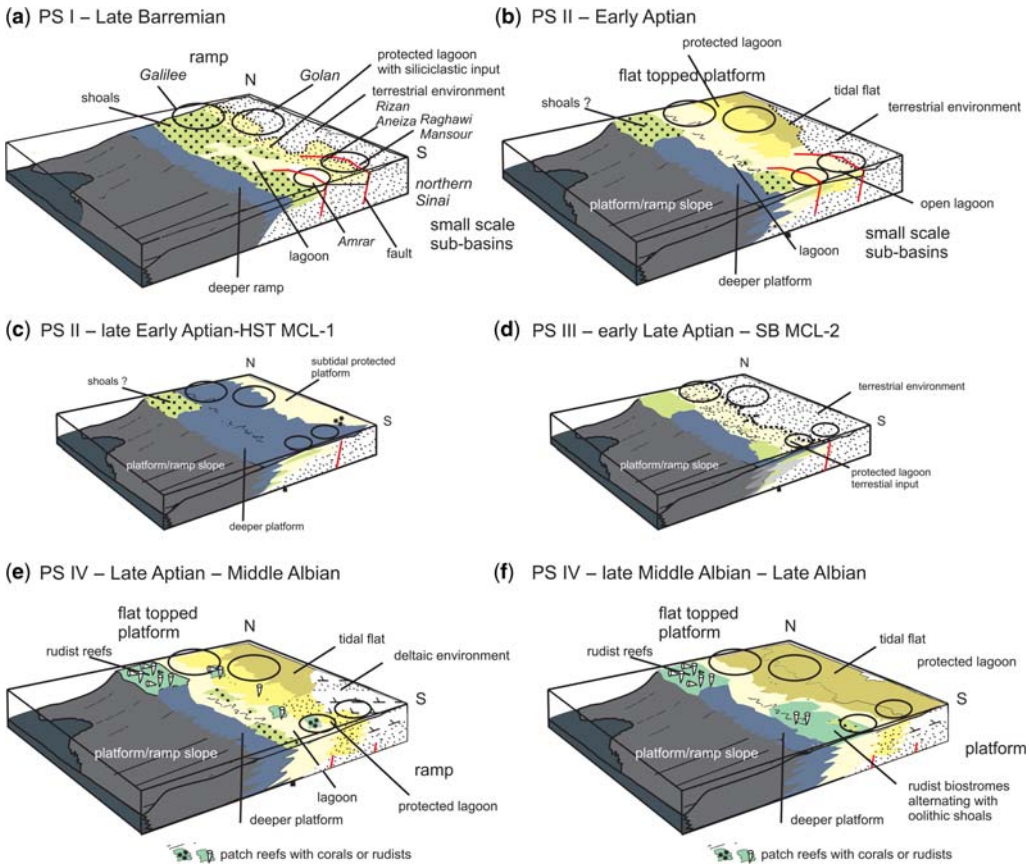


Fig. 9. Six models explaining the development of the depositional architecture of the Levant Platform in North Sinai and Galilee-Golan Heights area.

PS II. Limestones upward alternating with marlstones characterize the marine sediments of PS II.

PS II comprises the Ein El Assad Formation and the lower part of the Hydra Formation, corresponding to the Lower Aptian (upper LBFs *P1* and *Pc-O1*, Fig. 2) – lowermost Upper Aptian. At the boundary between PS I and PS II terrigenous input was interrupted and the lower part of PS II (Ein El Assad Formation) forms a prominent landmark of 55 m-thick pure limestones in Galilee and the Golan Heights. The upper part (lower Hydra Formation) crops out in the Golan Heights and is known from the subsurface only in the Galilee (Rosenfeld *et al.* 1998). Bioclastic packstones and wackestones of the Lower Ein El Assad Formation belong mainly to the low-energy open and protected lagoon FZs 3, 5 and 6 with high amounts of calcareous green algae in some layers (FZ 4). Intercalated are a few beds deposited under high-energy (FZ 2), restricted or tidal flat conditions (FZ 7). In the upper part of the Ein El Assad Formation increasing

open marine conditions are indicated by the occurrence orbitolinids-rich and planktic foraminifers-containing sediments of FZ 1 in all sections. Relatively uniform depositional conditions prevailed in the entire area with an only small gradient to more protected environments from west to east characterizing a homogenous shallow-platform environment reaching to an area west of the Golan area. Decreasing siliciclastic input of quartz and feruginous ooids indicate greater distance of the shoreline. The upper part of the Ein El Assad Formation (LFB *Pc-O1*) is characterized by a significant synchronous deepening event establishing deeper marine environments over the entire Galilee-Golan Heights region (Fig. 4). The onset of the Hydra Formation marks increasing terrigenous input. The siltstones, marlstone and limestone alternations were deposited in open-marine subtidal (FZ 3, 4) to protected environments (FZ 6 and 8). In the higher part of PS II shoaling and progradation of the coast line occur (Fig. 4).

PS III. Siliciclastic sediments characterize PS III in northern Israel.

PS III comprises 5 m of the middle part of the Hidra Formation, marked by fluvial sandstones of FZ 9 that can be not dated exactly. The underlying PS II extends at least into the late Early Aptian and the overlying PS VI is clearly related to the lower Upper Aptian. Thus, PS III is not older than late Early Aptian and not younger than early Late Aptian. PS III represents an important emergence horizon. A terrestrial facies can be proved from the Golan Heights, documenting the progradation of the coast line. Rosenfeld *et al.* (1998) described similar siliciclastic sediments of the Hidra Formation from the subsurface of the Galilee area, however without emergence. They describe a brackish facies from the Middle Hidra Formation indicating at least a near coast position for that region.

PS IV. PS IV comprises about an 150 m thick succession of marine marlstones and limestones.

It corresponds to the Upper Aptian to Middle Albian (LBFs *Op* and *Ot*, possibly *Os*) Rama Formation and is documented from the Golan Heights (Ein Quniya section) and from Galilee (Har Ramin section, Fig. 6a). The 45 m-thick limestone member forming the base of the lower Rama Formation (35 m at the Golan Heights) is characterized by often nodular bedded limestone deposited in the various FZs, reaching from open-marine deeper platform (FZ 1; only at Har Ramin) to tidal flat sediments (FZ 7) with a maximum occurrence of the open-marine shallow platform environments (FZ 3). Terrestrial input is low and rarely ferruginous ooids occur. The upper part of the Rama Formation is composed of limestone–marlstone alternations, mainly deposited in protected environments (FZs 5, 6 and 7) in Galilee and the Golan. Open lagoonal environments (FZ 3) occur only at Har Ramin. Slightly higher siliciclastic input of sand and marlstones occurs in the Lower Albian.

During deposition of the Rama Formation, the marine facies belt reaches again to an area significantly west of the Golan area. However, siliciclastic input of quartz and ferruginous ooids is still obvious. The facies indicates that a low-energy lagoon dominated the entire Formation, reaching from Golan Heights to Galilee, and limited to the west by fringing rudist bioherms at the Carmel area in the western Galilee (described by Sass & Bein 1982), and to the east by terrestrial deposits in Jordan.

PS V. PS V includes dolomites of the Yagur Formation and was analysed only at Har Ramin (Galilee), where pure dolomites reflect protected lagoon (FZ 6) and tidal flat deposition (FZ 7). According to Rosenfeld *et al.* (1998) a late Middle

Albian can be assumed. Similar sediments are described from cores in Galilee, from the Golan (Hirsch 1996), and from southern Israel (Rosenfeld *et al.* 1998; Rosenfeld & Hirsch 2005) indicating an enlarged shallow platform covering Israel.

Structural control on the Late Barremian–Albian deposits of the Levant Platform

The North Sinai record. Deposition of Early Cretaceous strata took place between Late Jurassic extensional and Late Cretaceous compressional tectonics. While the Late Jurassic extension resulted in predominantly NW dipping extensional normal faults (Moustafa & Khalil 1990; Garfunkel 1998), the Late Cretaceous compressional stage resulted in three fold ranges in North Sinai, owing to the inversion of the former extensional faults. The interpretation of the Late Barremian–Albian sedimentary record and the arrangement of facies belts in the palaeogeographical maps allow the reconstruction of extensional movements along these faults during Early Cretaceous times. Facies zones are generally orientated in WSW–ENE trending belts parallel to these major extensional faults (Figs 8 & 9).

The prominent anticlinal structure of Gebel Maghara lies at the northernmost fold range, in between east–NE elongated belts of right-stepping en-echelon folds, interpreted as representing the strike–slip rejuvenation of deep-seated earlier extensional faults (Moustafa & Khalil 1990).

Those reverse faults were observed at Gebel Amrar and Gebel Raghawi (Fig. 8g; compare Moustafa 2010), where abrupt facies and thickness changes of Early Cretaceous sediments across these faults indicate their importance during earlier extensional stages and might have been active until the early Late Aptian. The southern SW–NE trending fault (Raghawi–Mansour fault) separates the Raghawi and the Mansour areas with its lateral elongation further NE, at Rizan Aneiza. The Amrar section (Fig. 8f) is located at a second extensional SW–NE trending fault, again rejuvenated during the Upper Cretaceous compression (Amrar fold belt sensu, Moustafa & Khalil 1990). Two similar sets of faults with vertical movement were also described by Moustafa (2010).

The following sedimentological and stratigraphical observations suggest a structural control on Early Cretaceous deposition along normal faults of North Sinai.

- (1) The Upper Barremian to lower Upper Aptian (PS I–II) sections at the neighbouring Gebels Raghawi and Mansour (located *c.* 5 km apart) show significantly different sedimentary environments (Fig. 7). In the Mansour area, sedimentation took place under terrestrial

conditions, while more than 240 m of marly and limy sediments were deposited in marine environments at Gebel Raghawi. To interpret this record we either have to assume a primary, very steep, declining coast (with vertical differences of more than 200 m along a 5 km horizontal distance), or more probable, an active normal fault that resulted in higher subsidence rates in the northern areas. At the end of PS II (latest Early Aptian and earliest Late Aptian) water-depth at the Gebel Raghawi area increased significantly in contrast to still terrestrial environments at Gebel Mansour, and may thus reflect different subsidence owing to syndepositional tectonic activities along a normal fault. (Alternative interpretations of deposition and later erosion of marine sediments at Gebel Mansour seem unlikely because of missing reworking horizons). Our facies data hint on a SE–NW striking normal fault active during the Late Barremian–earliest Late Aptian (and reactivated in Late Cretaceous times), which caused the different depositional environments (Fig. 8f).

- (2) At Gebel Amrar, further to the NW, shallow marine Upper Barremian–lower Upper Aptian deposits indicate a swell, which may be correlated with another active normal fault belonging to the Amrar fold belt (Moustafa & Khalil 1990).

During PS III (early Late Aptian) terrestrial sedimentation occurred in the entire northern Sinai, which was accompanied by erosion in the southern sections (Fig. 8c). During PS IV (latest Aptian–Middle Albian) stepwise encroaching of the marine sediments from north–NW to south–SE indicates a slightly dipping ramp (Fig. 8d). Uniform sediments at Raghawi and Mansour characterize the next stage (PS V), with some beds traceable for long distances (Fig. 8e). This means that the Raghawi–Mansour fault was active only until the end of the Early Aptian, possibly until the earliest Late Aptian. During the younger stages (PS III) erosion and deposition reduced the former elevation gradient along the normal faults, until more homogenous depositional environments became obvious during PS IV (Fig. 8).

The sedimentological and stratigraphical data suggest extensional tectonical activity during the Barremian–Early Aptian, which is younger than described before (Garfunkel 1998; Moustafa & Khalil 1990; Moustafa *et al.* 1990). Only since the Late Aptian, subsequent to tectonical activity, a stepwise retrogradation took place and the facies development was controlled only by global sea-level change and supraregional tectonics.

The Galilee–Golan Heights structural development. The northern Israel Barremian–Albian structural development is much simpler as in North Sinai. During the Late Barremian, flooding of the terrestrial area created a slightly inclining ramp structure. Owing to different depositional rates, a landward-thinning wedge of sediments (described by Rosenfeld *et al.* 1998) filled the available accommodation space until a shallow, uniform platform developed during the Early Aptian (Bachmann & Hirsch 2006). Distally steepening of the ramp and a shelf break is suggested for the Carmel area, where rudist bioherms fringe the shelf-break and are closely allied to deeper marine sediments during the Albian period and deeper marine sediments were deposited nearby (Bein 1971; Sass & Bein 1982). This is confirmed by seismic profiles (Garfunkel 1998). In summary, we suggest a depositional regime, which was mainly controlled by sedimentation rates, sediment production, and sea-level changes without evident tectonic influence. Facies models for the Galilee–Golan Heights area include a post-depositional, Oligocene–recent sinistral strike–slip movement along the Jordan–Gulf of Aqaba line (Fig. 1b, e.g. Garfunkel & Ben-Avraham 1996; Flexer *et al.* 2005; Mart *et al.* 2005). The rate of sinistral displacement is controversially discussed, reaching from 10 km (Mart *et al.* 2005) to 110 km (Garfunkel & Ben-Avraham 1996; Gilat 2005). Our sections show no evidence for strong lateral displacement since displacement was parallel to facies belt boundaries.

Second-order sequences

Second-order sequences were already discussed for the Galilee–Golan area and for the upper part of the North Sinai succession (Bachmann *et al.* 2003; Bachmann & Hirsch 2006). Comparing both platform settings allow us to recognize second-order sequences that have controlled a large part of the Levant Platform.

We adopt three second-order sequences, formerly described from the Galilee–Golan Heights area and prefixed MC (mid-Cretaceous) EL (eastern Levant) and numbered (e.g. MCEL-1). For the larger extension of the analysed region, we transfer the prefix into MC (mid-Cretaceous) L (Levant) and add another sequence (Fig. 10).

MCL-1

In both areas, terrestrial sediments were flooded in the Late Barremian. For both areas, we document initial deepening and increasing accommodation during the Late Barremian–earliest Aptian, and at Galilee–Golan landward retrogradational patterns characterize the transgressive systems tract (TST).

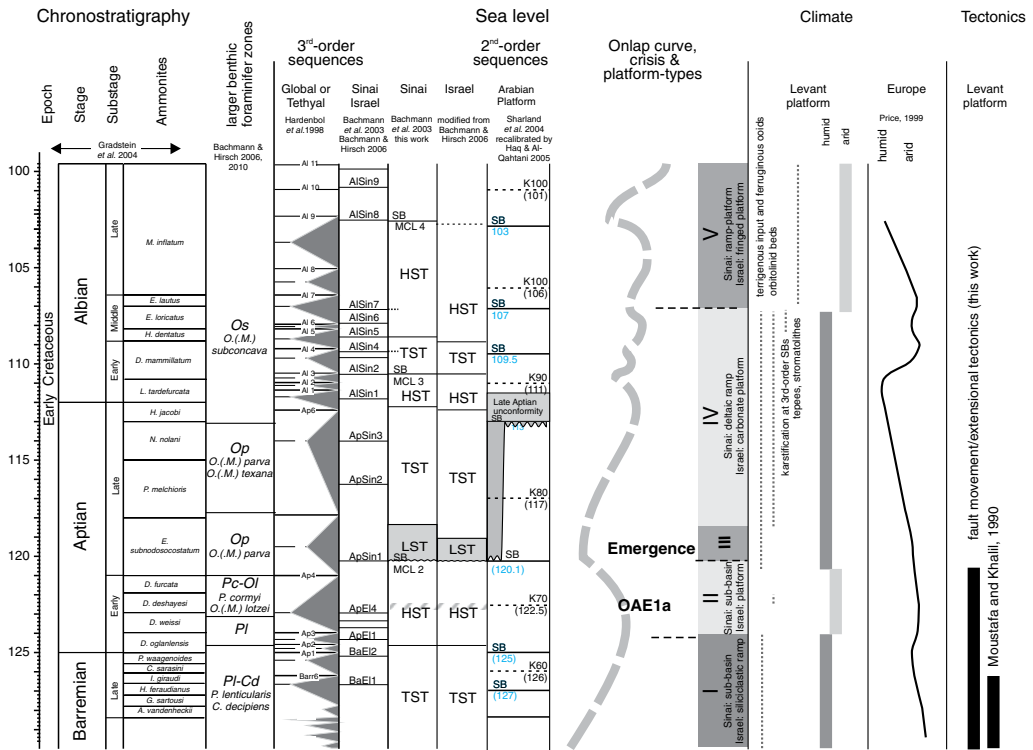


Fig. 10. Chronostratigraphic chart summarizing the stratigraphic and sequence stratigraphic interpretation, as well as the climate and tectonic data, in comparison with data on the Arabian Plate and the regions around the Tethys.

These retrogradation patterns were retarded in North Sinai, when the coastline reached the Raghawi area by the activity of the Raghawi–Mansour fault (Figs 7 & 8), while westward retrogradation crossed the Golan Heights without barrier (Fig. 4). The TST, characterized by high siliciclastic input and ferruginous ooid, was deposited under more or less open marine locally high-energy conditions (Fig. 4). A major change to low-energy inner platform conditions in the basal Lower Aptian marks the maximum-flooding surface (MFS) at the Galilee–Golan Heights. The early highstand systems tract (HST) comprises limestones deposited under lagoonal to open-marine conditions and the late HST more protected environments with increasing siliciclastic input (Fig. 4). No former southward transgression is documented and the creation of accommodation space is clearly reduced. In North Sinai, a steady coast line and a decrease in terrigenous input characterize the HST with a depositional environment clearly changing to open marine, deeper-shelf environments. However, no reduction of accommodation is documented, before the late HST, because of subsidence owing to local fault activity. In both areas an exceptional

third-order deepening event is observed superimposing the second-order HST, which largely correlates with the platform drowning observed at the Oceanic Anoxic Event 1a (Weissert *et al.* 1998; Bachmann & Hirsch 2006).

MCL-2

The sequence boundary (SB) of the MCL-2 is the most prominent emergence horizon in the entire succession, indicated by terrestrial sandstones which eroded into the underlying sediments (Sinai only, Fig. 4). For North Sinai the age of the SB can be dated as being earliest Late Aptian (Figs 3 & 4). In Israel it is recognized only in the Golan Heights, where its dating is unsure. Similarly pronounced is the transgressive surface (TS), when retrogradation of the facies belts is marked by the renewed marine sedimentation in both areas. During the TST, both areas are marked by increasing accommodation, retrograde submergence of the platform, and siliciclastic input (reduced in the late TST) in dominantly protected environments. Slightly higher accumulation at the Golan Heights, compared to North Sinai, may result from earlier

onset of the marine deposition. While at North Sinai the TS is dated as early Late Aptian [*C. (E.) subnodosocostatum* zone], the age is not confirmed yet for the Golan Heights. The basal Upper Aptian MFS is documented in the Golan area by the deepest environment in the study area, indicated by a sudden reduction in terrigenous input and followed by HST carbonates. The mfs in the North Sinai is interpreted as lying at a surface of re-establishment of carbonate dominated sediments (Raghawi and Rizan Aneiza sections), which coincides with a decrease of the southward transgression, indicated by interfingering of high-energy shoals at Raghawi with sediments of the proximal delta at Gebel Mansour.

The depositional rate of MCL-2 is slightly reduced compared to MCL-1, while the observed transgression to the south, especially at North Sinai, is much greater (Fig. 8g). However, observed depositional environments, which are generally characterized by shallower water-depth during MCL-2 indicates a general lower accommodation increase than before.

MCL-3

The Lower Albian SB MCL-3 is clearly defined at the Golan Heights (Ein Quniya section) and at Galilee (Har Ramin section) by a facies change from open marine to restricted environments (Fig. 4). At North Sinai, it is interpreted as lying below a distinct zone of delta progradation. The LST is indicated by terrigenous delta-influenced sediments in the northern distal sections and by coarse-grained sand dominated delta sediments in the proximal section M. The TSs are marked in both areas by deepening of the environment and by a clear trend to high-energy setting in the individual sections indicating increasing accommodation (Fig. 4). In North Sinai, prominent transgression during the TST results in submergence of the southern and eastern part of the Maghara area (section MgE, Fig. 8h). At Galilee the MFS is indicated by a significant change from open marine to protected environments under constant accommodation. At North Sinai, a change from consequent transgression to a succession with higher-frequency facies changes may result from reduced accommodation and mark the late Early Albian MFS. The HST in both areas is characterized by repeated siliciclastic input, but also by the development of rudist biostromes (North Sinai) or rudist debris fearing sediments (Galilee–Golan Heights).

MCL-4

The SB MCL-4 is marked by emergence in North Sinai and by facies change at Galilee (Fig. 4). The

Late Albian age confirmed at North Sinai may correlate with Galilee, where an accurate dating of the SB is not possible. In both areas, the LST contains few beds of intertidal dolomite. While only few intercalations of protected and open platform sediments mark the TST at Galilee, a succession with shoals, protected lagoons, and rudist biostromes dominate the TST at North Sinai. In the latter area the maximum flooding is characterized by the establishment of tidal flat sediments on large parts of the platform in the uppermost Upper Aptian. The uppermost part of the sequence is present in the Mansour north sections only; here the subsequent SB is of Early Cenomanian age.

Discussion

Platform development – geometry and facies development as a consequence of tectonics, siliciclastic input, production, and sea-level change.

The five platform-stages (I–V) reflect different depositional environments, accumulation patterns, and platform geometries (Fig. 9). We observe significant variations in one or more of the following parameters: tectonical activity, siliciclastic input (driven by climate and tectonics), carbonate production, and second-order sea-level. To chart the depositional models for the Levant Platform stages (Fig. 9) published subsurface data were incorporated, spanning the region between Galilee–Golan Heights and North Sinai.

PS I: Late Barremian–earliest Early Aptian. In both areas siliciclastic influenced carbonate sediments characterize the near shore environments, rich in ferruginous ooids and quartz (Fig. 9a). Marly sediments, with upward increasing carbonate content, are described from the central Israel hinge belt. A shallow water depositional environment was defined on the base of ostracod assemblages, with intercalated fresh-water signals, observed in central and northern Israel (Rosenfeld *et al.* 1998).

A strongly increasing sea level (TST MCL-1) resulted in transgression. Different subsidence, basic geometric regimes, and tectonical influence resulted in different depositional regimes in Sinai and Israel. At North Sinai, low-energy sub-basins developed between active normal faults, which caused enhanced subsidence rates, a stable coast line, and phases of higher siliciclastic input owing to higher-frequency sea-level changes. Sedimentological and tectonical data additionally indicate the existence of a swell in the northernmost part of the Sinai (Gebel Ambra region, Fig. 8) causing a low-energy depositional regime south of the swell with shallow and deeper lagoonal environments interrupted by sporadical coastal progradation. Those

features result in small-scaled variation of the sedimentation rates, with high sediment accumulation in front of the normal fault at Gebel Raghawi and low in the area south. We suggest a shelf break situated only a few kilometres north of the studied area, possibly linked with normal faults further north. This fits with deeper marine marls characterizing the offshore area only 20 km north of the studied sections at Rizan Aneiza (Martinotti 1993) and the occurrence of phylloceratid ammonites in the Lower Aptian sediments probably suggesting that deeper marine conditions were present in an area close to the studied ramp sediments (Lehmann *et al.* 2007). However, an odd taphonomic history has been suggested for this group of ammonites, with surfacing and floating of shells first that is followed by resinking by cameral puncture, and therefore a substantiation of an autochthonous origin can be complex (Maeda & Seilacher 1996). In northern Israel–Galilee, sediments form an eastward thinning wedge (Rosenfeld *et al.* 1998; Rosenfeld & Hirsch 2005), with more restricted environments in the eastern part (Fig. 9a). There is no sign of active faulting and sea-level rise result in gradual flooding of the former terrestrial sediments, with a coastline moving from the Galilee to east of the Golan Heights (Bachmann & Hirsch 2006). At Galilee a thick succession of high-energy grainstones indicate increasing accommodation. Gradual transgression and the landward increasing protection of the environments suggest a shallow ramp geometry with a huge high-energy facies belt. During the entire succession a continuous input of detrital components and ferruginous ooids indicates a humid weathering regime, confirmed by the intercalations of freshwater ostracod assemblages (Rosenfeld *et al.* 1998).

PS II: Early Aptian–earliest Late Albian. During the Early Aptian (HST MCL-1) both platform areas pass through significant changes; coarse-grained siliciclastic input is reduced, and thus carbonate dominates the submerged part of the platform (Fig. 9b). In the Galilee–Golan Heights and North Sinai, low-energy environments rich in calcareous algae and bioclasts occur. In the Galilee–Golan Heights, only slight lateral facies variations in large parts of the proximal platform indicate a large extension of the low-energy open-platform facies belt with similar water depths. Thus, flat-topped platform geometry was suggested to form homogenous shallow platform environments at the beginning of PS II. The seaward margin of this platform is not exposed in the studied area and rudist fringing reefs found in the Carmel area (30 km west of Galilee sections) were documented from younger successions only (Bein 1971; Sass & Bein 1982).

In North Sinai no change of the depositional geometry occurs compared to PS I. The Mansour–Raghawi fault and the Gebel Amrar swell controlled the depositional processes within the small sub-basin. In between Sinai and Galilee the subsurface descriptions indicate a transitional zone, without a major shelf break (Rosenfeld *et al.* 1998).

Deepening in the late Early Aptian starts with a succession of orbitolinid beds, followed by open-marine, deeper platform, marly sediments in both areas (Fig. 9c). This deepening causes a short-termed southward transgression exceeding the Mansour–Raghawi fault until the southwestern Maghara area and may reach into southern Negev (southern Israel), where short-termed marine transgressions is known from the Lower Aptian (*Deshayesites deshayesi* and *D. forbesi* ammonite zones) dated by fossils and radiometric ages of an overlying basalt (Gvirtzman *et al.* 1996).

PS III: Earliest Late Aptian. This short-termed platform stage marks a major break in the North Sinai depositional geometry, but is characterized by short-termed emergence in the Galilee–Golan Heights only (Fig. 9d). At North Sinai, the fault controlled differential subsidence patterns terminated and the sub-basins were filled with near shore and erosional deposits. Moreover, terrestrial (Raghawi), marine sandstones (Rizan Aneiza), and dolomites (Amrar) correlate with a major second-order lowstand. Regression is also marked by a northward movement of the coastline to an area in between Raghawi and Amrar (Fig. 9d). Erosional unconformities observed at Gebel Raghawi are possibly owing to denudation of the relief around the normal fault (Fig. 8) and may have shaped the initial stage of a low dipping ramp geometry (observed in the subsequent platform stages). Fluvial sandstones deposited at the Golan Heights indicate a major regression in the northeastern part of the study area. However, erosion was not observed and the geometry persisted homogenous. Altogether PS III presents a stage characterized by a widely emerged platform with distinct regression.

PS IV: Late Aptian–Middle Albian. The Late Aptian–Middle Albian PS IV comprises second-order sequence MCL-2 and the LST and TST of MCL-3, in both areas characterized by temporarily detrital influenced carbonate production. The platform was widely submerged and a gradual transgression marked the entire area (Fig. 9e).

At North Sinai, the transgression submerged the Rizan Aneiza, Amrar, Raghawi, and Mansour regions during Late Aptian and the southeastern part of the Maghara area during the Lower Albian (Fig. 7). First marine sediments occur 20 km south of Maghara at the end of PS IV (Bachmann *et al.*

2003). A broad delta system developed, which strongly influenced the depositional processes at Mansour and Maghara SE area interfingering with marine marl and limestones around Gebel Raghawi, while Rizan Aneiza was only slightly influenced by siliciclastic deltaics (Fig. 8g). A north dipping ramp geometry is indicated by increasing thickness of open marine sediments with rudist patch reef, oolitic shoals, and lagoonal sediments towards the north. This gradient was considerably developed at the end of PS IV, when mid-ramp environments at Rizan Aneiza gradually passed into lagoons at Raghawi. The dipping direction changed from NW during PS I–III to N (NNW) during PS IV, triggered by the deltaic input from the southern direction. The ramp can be subdivided in three main facies belts: a southern deltaic depositional facies (Mansour and Maghara SE), a shallow protected subtidal facies (Raghawi), and an open subtidal facies with rudist patch reefs in the north (Rizan Aneiza, Fig. 8g). Those facies belts prograded and retrograded following higher frequency sea-level changes. The extensive siliciclastic input in the delta realm caused higher sedimentation rates in the proximal parts of ramp. Only in the upper PS IV did the depocentre move towards north–NW, when the proximal platform was emerged during the third-order LSTs of the early second-order HST of MCL-3 and sedimentation rates increased in the more distal parts of the platform.

At Galilee–Golan Heights the entire platform was submerged since the Late Aptian. Marine sedimentation in the adjacent Jordan is not older than latest Albian (e.g. Schulze *et al.* 2004), which indicates that the coastline was close to the Golan Heights. Rudist fringing reefs were established at the shelf hinge (Bein 1971; Sass & Bein 1982). Ross (1992) pointed out that the back reef gravel may have formed a major hydrologic barrier, while Bein & Weiler (1976) documented the lower slope nature of muddy sediments deposited in close vicinity to the fringing reefs at the Carmel area. Homogenous flat-topped platform geometry and a strong decrease in hydrologic energy in the proximal platform areas resulted in a shallow lagoonal inner platform environment that varied little over a large area. Sedimentation rates were very similar in the inner platform area, comprising Galilee and the Golan Heights. In the area in between Sinai and northern Israel, a facies established similar to the northern region (Rosenfeld & Hirsch 2005).

PS V: Late Albian. PS V is characterized by gradual change of the platform geometry at Sinai and constant filling of the accommodation at Galilee and Golan Heights (Fig. 9f). PS V comprises the last

herein studied second-order sequence. In both areas sediments of the protected inner platform area with strong reduced siliciclastic amounts are prevailing. Crucial for the development of North Sinai was the dislocation of the rising sea-level. The sedimentation rates increased in the more distal sections resulting in filling of distal accommodation. A very homogenous flat-topped platform developed. During the Late Albian this platform extended southwardly to an area 100 km south of Maghara (Bachmann & Kuss 1998). Within this large extended platform, a succession of rudist biostromes, alternating with protected lagoonal and algal-laminate dominated tidal flats, were deposited resulting from higher frequency sea-level changes. Deposition of grainstones and oolitic facies was restricted to short intervals at Gebel Raghawi, indicating the low-energy dominance during that interval and suggesting a shelf break in an area further north.

In Galilee, dolomites representing tidal flats and lagoon prevail, which are also described from the Golan Heights and from Judea in between Galilee and North Sinai (Rosenfeld & Hirsch 2005).

The Upper Albian distribution of facies belts indicates a large extended homogenous, very shallow, platform without major changes in facies reaching from northern Israel and the Golan Heights to North Sinai. A continuously increasing sea-level resulted in high accumulation rates and southward transgression. However, platform growth kept up with the sea-level rise and shallow-water, and intertidal deposition continued.

External controlling factors

As external factors controlling the sedimentation patterns on the carbonate platform we consider climate and global sea-level changes. Imprints of those changes should occur at both platform areas studied, independent from different tectonical regimes, and are comparable to similar changes observed on other Tethyan platforms (Fig. 10).

Second-order sea-level change and its influence on the formation of the platform stages. Second-order sea-level changes highly influenced the Levant platform development by controlling the accommodation and the centres of deposition. During the Late Barremian–Early Aptian a second-order TST created the accommodation to start up the marine sedimentation. Reduced accommodation during second-order HST resulted in distal dislocation of the depocentre and thus controlled the replacement of the ramp by flat topped platform architecture in Galilee–Golan Heights. Erosion during the early Late Aptian LST (SB MCL-2) influenced the ramp

geometry in North Sinai, while reduced accommodation during MCL-3 HST and MCL-4 LST initially induced the distal dislocation of the depocentre and the change from ramp to platform architecture in North Sinai.

A comparison of global sequences with that of the Arabian plate origin is shown in Figure 10. Data are constrained by the stratigraphical frame slightly clouded by the use of different time scales in the several studies. The southern Arabian plate exhibit similar features concerning the widespread continental siliciclastic sediments flooded during the Late Barremian, and marine sedimentation during Aptian–Albian times (Haq & Al-Qahtani 2005; Sharland *et al.* 2001, Fig. 10). The early Late Aptian sequence boundary (MCL-2) coincides with prominent sequence boundaries observed at various localities of the Arabian plate (Van Buchem *et al.* 2002; Gréselle & Pittet 2005; Haq & Al-Qahtani 2005). A second match with the Arabian plate feature is observed for the Late Aptian SB MCL-4, while SB MCL-3 is younger than that observed on the southern Arabian plate (Gréselle & Pittet 2005; Haq & Al-Qahtani 2005). Some further second-order SBs observed on the southern Arabian plate by Gréselle & Pittet (2005) or Haq & Al-Qahtani (2005) coincides with SBs regarded as a higher frequency in origin in North Sinai, because they are not clearly indicated at Galilee–Golan Heights. Important differences to the southern Arabian plate were observed in the Upper Aptian succession. While a Late Aptian unconformity is documented from several platforms (Van Buchem *et al.* 2002; Haq & Al-Qahtani 2005), continuous marine sedimentation took place in the Levant Platform at the northern edge of the Arabian plate.

Comparing the sea-level changes with patterns supposed to be global, similarities are much less obvious. However, the transgression characterizing the Upper Aptian–Albian Levant succession coincides with the long-term global transgression pointed out by Hardenbol *et al.* (1998), while the lower part of the succession falls into a global sea-level minimum. This agrees with transgressions of smaller amplitude during that time interval on the Levant Platform. Additionally SB MCL-2 possibly correlates with Ap 4 defined by Hardenbol *et al.* (1998) and with a few time-equivalent exceptional SBs in the northern Tethyan realm, like the Alpine mountains (e.g. Roter Sattel, Strasser *et al.* 2001), while other areas are characterized by transgression or high stand during the same time.

Altogether, the sea-level history of the Levant Platform reflects the Late Aptian–Albian global long-term transgression and the second-order sea-level changes are highly correlated with that one observed on the Arabian plate.

Climate. The composition of the siliciclastic input and the formation of ferruginous ooids allow the interpretation of general climate conditions in the study area (Fig. 10). The Upper Barremian–Albian succession comprises two intervals with coarse grained siliciclastic input and occurrence of ferruginous ooids, one reaches from the Late Barremian to the earliest Aptian (PS I) and the second comprises the Late Aptian until the mid-Albian (PS IV). Within these parts of the succession marly facies dominates and carbonatic samples often show a marly matrix. These intervals were interpreted as indicating humid conditions (Bachmann & Hirsch 2006; Bachmann & Kuss 1998) in concordance with Mücke (2000), who demonstrated that lateritic weathering in the hinterland was producing the protoliths for Upper Cretaceous oolitic ironstones. Those interpretations are underlined by the common occurrence of plant remains in the succession of PS I at Gebel Raghawi and by the formation of the pronounced delta system and carstification horizons in North Sinai during PS IV. Orbitolinid-rich facies types, associated with abundant calcareous algae and echinoderms and argillaceous muddy limestones, are common in PS IV. Those facies types are typically interpreted as reflecting mesotrophic conditions (Van Buchem *et al.* 2001; Pittet *et al.* 2002), which may reflect nutrient input owing to weathering and humid conditions.

Two intervals are characterized by reduced siliciclastic input and the absence of the ferruginous ooids (Early Aptian/PS II and the Late Albian/PS V). Such a reduced siliciclastic input can result from reduced sediment supply owing to less intensive weathering or from an increasing distance of the delivery area. For PS II, the steady coast line between Mansour and Raghawi during lower PS II argues for a climate origin of the reduction of detrital input. The Late Albian (PS V) of reduced siliciclastic input is accompanied by an increase of rudist and miliolid dominated pure limestones in North Sinai. Those facies types are commonly interpreted as reflecting oligotrophic conditions (Van Buchem *et al.* 2002), which fit well with the observed transgressional, less humid system.

Changing third-order low stand features accompany humid and less humid phases. LSTs are characterized by detrital input during the humid phases and by emergence and dolomitization during the less humid periods (Bachmann & Kuss 1998).

Our data fit with the general ideas of Price (1999) and Hillgärtner *et al.* (2003) for the Oman, who indicated a small trend to humidity in the Late Barremian–Early Aptian. However, the position of the Levant Platform near the equator may have triggered humidity in northeastern Africa, while more

arid conditions influence the northern Tethyan margin during the Barremian–earliest Aptian.

Tectonics. Tectonical activity played an important role, especially during the initial phase of the platform development in North Sinai (Fig. 10). Our data suggest that during the Late Barremian–Early Aptian, extensional normal faults influenced the North Sinai environment and result in the formation of sub-basins, while at the same time a slightly dipping ramp, without fault segmentation, is recorded in northern Israel. The Late Aptian–Albian distribution of the facies belts in North Sinai indicates a uniform deepening in a NW direction and confirms that sedimentation geometry was orientated parallel to SW–NE striking normal faults pointed out by Moustafa & Khalil (1990). Pre-deposition extensional tectonics creating normal faults are described from the Levant margin offshore Israel as well as from northern Sinai until the mid-Jurassic (Moustafa & Khalil 1990; Garfunkel 2004; Gardosh & Druckman 2006). In North Sinai, a set of extensional basins was created from which the Maghara area represents the northernmost point that was located onshore (Moustafa 2010). Extensional tectonics at the North African–Arabian continental margin are interpreted as reflecting divergent movement between the Afro-Arabian and the Eurasian plate, which led to the Mesozoic to Middle Jurassic opening of the Neotethys (Stampfli *et al.* 2001). Our data indicate that extensional faults were active until the late Early Aptian in North Sinai and may represent a Lower Cretaceous syn-rift stage according to Guiraud *et al.* (2005), who observed continental rifts along the African–Arabian Tethyan margin in the Late Berriasian–earliest Aptian.

Conclusions

During the Late Barremian–Albian, the southern Levant Platform was studied in the two regions: northern Israel (Galilee–Golan Heights) and North Sinai. Facies, stratigraphy and stable isotopes of several sections were studied, to reconstruct transects across the shallow shelf. In conclusion we establish depositional models and discuss the controlling factors for the shallow water deposition.

We combined biostratigraphy on the base of benthic foraminifers, mainly orbitolinids, and ammonites with stable isotope data, which allow us to date the shallow water strata and all controlling factors in detail. The depositional architecture was controlled by local tectonics, climate, and second-order sea-level changes affecting the sedimentation patterns. Four second-order sequence boundaries were identified in the Levant area (MCL-1–MCL-4). They partly

correlate with those observed on the Arabian plate (Haq & Al-Qahtani 2005; Sharland *et al.* 2001), suggesting a regional control. Until the late Early Aptian, the North Sinai was influenced by normal fault development, while the Galilee area–Golan Heights exhibit continuous sedimentation without tectonical influence.

Both regional transects reveal five platform stages (PS I–V) that differs with respect to platform architecture, siliciclastic input, and response to sea-level changes.

PS I (Late Barremian–earliest Aptian). The Upper Barremian marine sediments transgraded on terrestrial deposits. In northern Israel a homogenous ramp existed, while North Sinai was subdivided in SW–NE striking sub-basins, marginally bounded by active normal faults. Open marine high-energy sedimentation and continuous transgression characterized the Galilee–Golan Heights area during the TST of MCL-1, while near coast siliciclastic and protected lagoonal carbonates alternate with deeper marine sediments in North Sinai.

PS II (Early Aptian–earliest Late Aptian). During the HST of MCL-1, continuous filling of the accommodation resulted in shallow marine protected facies belts marking flat-topped platform architecture at northern Israel. Owing to higher subsidence around normal faults, sub-basin development kept on in North Sinai. The sedimentation was characterized by protected–partly deeper–subtidal environment within these sub-basins, separated from each other by shallower swells. Significant reduction of detrital input in both areas may result from changing weathering regimes.

PS III (early Late Aptian). During the LST of MCL-2 the tectonical activity terminated resulting in reorganization of the North Sinai platform. The former fault-controlled sub-basins became inactive and were covered by a shallow ramp architecture that controlled the depositional processes of the western Levant Platform. Emergence was evidenced from North Sinai to northern Israel indicating an extended platform system.

PS IV (Late Aptian–Middle Albian). A stable platform architecture, marked by a homoclinal ramp in North Sinai and a flat-topped platform in Galilee–Golan Heights, was sandwiched between transgressive surface MCL-2 and the end of TST of MCL-3. In the North Sinai a broad delta system with high siliciclastic input was deposited, interfingering in the north with carbonate ramp deposits. High accumulation rates on parts of the ramp resulted in slight changes of the dipping direction. Simultaneously,

a less siliciclastic input and inner platform sediments are characterized in the Galilee–Golan Heights region.

PS V (Late Albian and younger). During HST of MCL-3 and TST of MCL-4 pure limestones and dolomites were accommodated in North Sinai, during the ongoing transgression a flat topped platform was established here as well as in northern Israel.

Our data indicate that extensional faults controlled sedimentation until the late Early Aptian, which is significantly younger than observed before (Moustafa & Khalil 1990; Garfunkel 2004; Gardosh & Druckman 2006). They may represent a syn-rift stage according to Guiraud *et al.* (2005).

Concerning the climate history, we point out that the larger input of detrital sediment, including ferruginous ooids, indicates an increased humidity owing to an accelerated continental weathering, particularly in the Late Barremian–Early Aptian.

We are indebted to F. Hirsch (Jerusalem) and R. Stein (Bremerhaven) for discussions on the Lower Cretaceous of Israel, respectively geochemical data. We are especially thankful for J. Thielemann (Bremen) and M. Heldt (Hannover) for assistance in the field, many successful discussions, and providing valuable data of their theses. A. R. Moustafa (Cairo) helped with discussing the tectonical background of the working-areas. Technical support by M. Krogmann (Bremen) is appreciated for preparing a part of the ammonite fauna. We thank the two reviewers M. Simmons and R. Scott for helpful and instructive discussions and comments. We appreciate financial support by the German Science Foundation and the VW foundation.

References

- ABOUL ELA, N. M., ABDEL GAWAD, G. L. & ALY, M. F. 1991. Albian fauna of Gabal Manzour, Maghara area, north Sinai, Egypt. *Journal of African Earth Sciences*, **13**, 201–220.
- ABU-ZIED, R. H. 2007. Palaeoenvironmental significance of Early Cretaceous foraminifera from northern Sinai, Egypt. *Cretaceous Research*, **28**, 765–784.
- ABU-ZIED, R. H. 2008. Lithostratigraphy and biostratigraphy of some Lower Cretaceous outcrops from Northern Sinai, Egypt. *Cretaceous Research*, **29**, 603–624.
- AGUADO, R. & COMPANY, M. 1997. Biostratigraphic events at the Barremian/Aptian boundary in the Betic Cordillera, southern Spain. *Cretaceous Research*, **18**, 309–329.
- ARKIN, Y., BARTOV, Y. & GOLDBERG, M. 1975. The Geology of Rizan Aneiza, Northern Sinai. *Internal Report*, No. MM 2/75, 1–19.
- ARNAUD-VANNEAU, A. 1998. (Coord. L. Cret.). Larger benthic foraminifera. In: HARDENBOL, J., JACQUIN, T., FARLEY, M. B., DE GRACIANSKY, P.-C. & VAIL, P. (eds) *Cretaceous Biostratigraphy*, chart 5.
- ARNAUD-VANNEAU, A. & ARNAUD, H. 1990. Hauterivian to Lower Aptian carbonate shelf sedimentation and sequence stratigraphy in the Jura and northern Subalpine chains (southeastern France and Swiss Jura). *Special Publication, International Association of Sedimentologists*, **9**, 203–233.
- ARNAUD, H., ARNAUD-VANNEAU, A. *ET AL.* 1998. Répartition stratigraphique des orbitolinidés de la plate-forme urgonienne subalpine et jurassienne (SE de la France). *Géologie Alpine*, **74**, 3–89.
- ASKALANY, M. M. & ABU-ZEID, K. A. 1994. Contribution to the geology of El-Amrar and Rizan Aneiza areas, Northern Sinai (Egypt). *Bulletin of the Faculty of Sciences Assiut University*, **23**, 81–99.
- BACHMANN, M., BASSIUNI, M. A. A. & KUSS, J. 2003. Timing of mid-Cretaceous carbonate platform depositional cycles, northern Sinai, Egypt. *Palaeogeography, Palaeoclimatology, Palaeoecology*, **200**, 131–162.
- BACHMANN, M. & HIRSCH, F. 2006. Lower Cretaceous carbonate platform of the eastern Levant (Galilee and the Golan Heights) – stratigraphy and second-order sea-level change. *Cretaceous Research*, **27**, 487–512.
- BACHMANN, M. & KUSS, J. 1998. The Middle Cretaceous carbonate ramp of the northern Sinai: sequence stratigraphy and facies distribution. In: WRIGHT, V. P. & BURCHETTE, T. P. (eds) *Carbonate Ramps*. Geological Society, London, Special Publications, **149**, 253–280.
- BARTOV, Y. & STEINITZ, G. 1977. The Judea and Mount Scopus Groups in the Negev and Sinai with Trend Surface Analysis of the thickness data. *Israel Journal of Earth Science*, **28**, 119–148.
- BEIN, A. 1971. Rudist reef complexes (Albian to Cenomanian) in the Carmel and the coastal plain, Israel. *Geological Survey of Israel Report*. 86.
- BEIN, A. & WEILER, Y. 1976. The Cretaceous Talme Yafe formation: a contour current shaped sedimentary prism of calcareous detritus at the continental margin of the Arabian Craton. *Sedimentology*, **23**, 511–532.
- BERNAUS, J. M., ARNAUD-VANNEAU, A. & CAUS, E. 2002. Stratigraphic distribution of Valanginian–Early Aptian shallow-water benthic foraminifera and algae, and depositional sequences of a carbonate platform in a tectonically-controlled basin: the Organyà Basin, Pyrenees, Spain. *Cretaceous Research*, **23**, 25–36.
- BERNAUS, J. M., JOSEP, M., ARNAUD-VANNEAU, A. & CAUS, E. 2003. Carbonate platform sequence stratigraphy in a rapidly subsiding area; the late Barremian–early Aptian of the Organya Basin, Spanish Pyrenees. *Sedimentary Geology*, **159**, 177–201.
- BRAUN, M. & HIRSCH, F. 1994. Mid Cretaceous (Albian–Cenomanian) carbonate platforms in Israel. *Cuadernos de Geología Iberia*, **18**, 59–81.
- CASEY, R. 1962. A monograph of the Ammonoidea of the Lower Greensand. Part IV. *Palaeontographical Society Monographs*, **116**, 217–288.
- CASEY, R., BAYLISS, H. M. & SIMPSON, M. 1998. Observations on the lithostratigraphy and ammonite succession of the Aptian (Lower Cretaceous) Lower Greensand of Chale Bay, Isle of Wight, UK. *Cretaceous Research*, **19**, 511–535.

- CASTRO, J. M., COMPANY, M., DE GEA, G. A. & AGUADO, R. 2001. Biostratigraphy of the Aptian-Middle Cenomanian platform to basin domain in the Prebetic Zone of Alicante, SE Spain: calibration between shallow water nectonic and pelagic scales. *Cretaceous Research*, **22**, 145–156.
- CLAVEL, B., CHAROLLAIS, J., SCHROEDER, R. & BUSNARDO, R. 1995. Réflexions sur la biostratigraphie du Crétacé inférieur et sur sa complémentarité avec l'analyse séquentielle: exemple de l'Urgonien jurassien et subalpin. *Bulletin de la Société Géologique de France, Huitième Série*, **166**, 663–680.
- CONRAD, M. A., SCHROEDER, R., CLAVEL, B., CHAROLLAIS, J., BUSNARDO, R., CHERCHI, A. & DECROUEZ, D. 2004. Dating the Lower Cretaceous in the Organyà section (Catalan Pyrenees, NE Spain): a reinterpretation. *Cretaceous Research*, **25**, 35–41.
- DE GEA, G. A., CASTRO, J. M., AGUADO, R., RUIZ, P. A. & COMPANY, M. 2003. Lower Aptian carbon isotope stratigraphy from distal carbonate shelf setting: the Cau section, Prebetic zone, SE Spain. *Palaeogeography, Palaeoclimatology, Palaeoecology*, **200**, 207–219.
- DELANOY, G. 1997. Biostratigraphie des faunes d'Ammonites à la limite Barrémien-Aptien dans la région d'Angles-Barrême-Castellane. Étude particulière de la famille des Heteroceratina Spath, 1922 (Ancyloceratina, Ammonoidea). *Annales du Muséum d'Histoire Naturelle de Nice*, **12**, 1–270.
- DELANOY, G. & EBBO, L. 2000. Une nouvelle espèce d'*Heteroceras*: *H. mascarelli* sp. nov. (Ancyloceratina, Ammonoidea) dans le Barrémien du Sud-Est de la France. *Annales du Muséum d'histoire Naturelle de Nice*, **15**, 1–17.
- EL-ARABY, A.-M. 1999. Facies analysis and sequence stratigraphy of the Late Aptian–Albian Risan Aneiza Formation in northern Sinai, Egypt. *Egyptian Journal of Geology*, **43**, 151–180.
- ELIEZRI, I. Z. 1965. The Geology of the Beit-Jann region (Galilee, Israel). *Israel Journal of Earth Science*, **14**, 51–66.
- FLEXER, A., HIRSCH, F. & HALL, S. H. 2005. Tectonic Evolution of Israel. In: HALL, J. K. ET AL. (eds) *Geological Framework of the Levant. Volume II: The Levantine Basin and Israel*. Jerusalem: Historical Productions–Hall, 523–538.
- FÖLLMI, K. B., GODET, A., BODIN, S. & LINDER, P. 2006. Interactions between environmental change and shallow water carbonate buildup along the northern Tethyan margin and their impact on the Early Cretaceous carbon isotope record. *Paleoceanography*, **21**, 1–16.
- GALE, A. S., KENNEDY, W. J., BURNETT, J. A., CARON, M. & KIDD, B. E. 1996. The Late Albian to Early Cenomanian succession at Mont Risou near Rosans (Drôme, SE France): an integrated study (ammonites, inoceramids, planktonic foraminifera, nannofossils, oxygen and carbon isotopes). *Cretaceous Research*, **17**, 515–606.
- GARDOSH, M. A. & DRUCKMAN, Y. 2006. Seismic stratigraphy, structure and tectonic evolution of the Levantine Basin, offshore Israel. In: ROBERTSON, A. H. F. & MOUNTRAKIS, D. (eds) *Tectonic Development of the Eastern Mediterranean Region*. Geological Society, London, Special Publications, **260**, 201–227.
- GARCÍA-MONDÉJAR, J., OWEN, H. G., RAISOSSADAT, S. N., MILLÁN, M. I. & FERNÁNDEZ-MENDIOLA, M. A. 2009. The Early Aptian of Aralar (northern Spain): stratigraphy, sedimentology, ammonite biozonation, and OAE1. *Cretaceous Research*, **30**, 434–464.
- GARFUNKEL, Z. 1998. Constraints on the origin and history of the Eastern Mediterranean basin. *Tectonophysics*, **298**, 5–35.
- GARFUNKEL, Z. 2004. Origin of the Eastern Mediterranean basin: a reevaluation. *Tectonophysics*, **391**, 11–34.
- GARFUNKEL, Z. & BEN-AVRAHAM, Z. 1996. The structure of the Dead Sea basin. *Tectonophysics*, **266**, 155–176.
- GILAT, A. 2005. Strike-slip faulting west of the Dead Sea Escarpment. In: HALL, J. K., KRASHENINNIKOV, V. A., HIRSCH, F., BENJAMINI, CH. & FLEXER, A. (eds) *Geological Framework of the Levant. Volume II: The Levantine Basin and Israel*. Jerusalem: Historical Productions–Hall, 515–522.
- GODET, A., BODIN, S. ET AL. 2006. Evolution of the marine stable carbon-isotope record during the early Cretaceous: a focus on the late Hauterivian and Barremian in the Tethyan realm. *Earth and Planetary Science Letters*, **242**, 254–271.
- GRÉSELLE, B. & PITTET, B. 2005. Fringing carbonate platforms at the Arabian Plate margin in northern Oman during the Late Aptian–Middle Albian: evidence for high-amplitude sea-level changes. *Sedimentary Geology*, **175**, 367–390.
- GUIRAUD, R., BOSWORTH, W., THIERRY, J. & DELPLANQUE, A. 2005. Phanerozoic geological evolution of Northern and Central Africa: an overview. *Journal of African Earth Sciences*, **43**, 83–143.
- GVIRTZMAN, G., WEISSBROD, T., BAER, G. & BRENNER, G. J. 1996. The age of the Aptian stage and its magnetic events: new Ar–Ar ages and palaeomagnetic data from the Negev, Israel. *Cretaceous Research*, **17**, 293–310.
- HAQ, B. U. & AL-QAHTANI, A. M. 2005. Phanerozoic cycles of sea-level change on the Arabian Platform. *GeoArabia*, **10**, 127–160.
- HARDENBOL, J., JACQUIN, T., FARLEY, M. B., DE GRACIANSKY, P. C. & VAIL, P. R. 1998a. Mesozoic and Cenozoic sequence chronostratigraphic framework of European basins. In: DE GRACIANSKY, P. C., HARDENBOL, J., JACQUIN, T. & VAIL, P. R. (eds) *Mesozoic and Cenozoic Sequence Stratigraphy of European Basins*. Society for Sedimentary Geology (SEPM), Tulsa, 3–13.
- HARDENBOL, J., THIERRY, J., FARLEY, M. B., THIERRY, J., DE GRACIANSKY, P.-C. & VAIL, P. R. 1998b. Cretaceous sequence chronostratigraphy – Mesozoic and Cenozoic sequence chronostratigraphical framework of European basins. In: DE GRACIANSKY, P.-C., HARDENBOL, J., JACQUIN, T. & VAIL, P. R. (eds) *Mesozoic and Cenozoic Sequence Stratigraphy of European Basins*. Society for Sedimentary Geology (SEPM), Tulsa, Chart 5.
- HEIMHOFER, U., HOCHULI, P. A., HERRLE, J. O., ANDERSEN, N. & WEISSERT, H. 2004. Absence of major vegetation and palaeoatmospheric pCO₂ changes associated with oceanic anoxic event 1a (early Aptian, SE France). *Earth and Planetary Science Letters*, **223**, 303–318.
- HELDT, M., BACHMANN, M. & LEHMANN, J. 2008. Microfacies, biostratigraphy, and geochemistry of the

- hemipelagic Barremian–Aptian in north-central Tunisia: Influence of the OAE1a on the southern Tethys margin. *Palaeogeography, Palaeoclimatology, Palaeoecology*, **261**, 246–260.
- HILLGÄRTNER, H., VAN BUCHEM, F. S., GAUMET, F., RAZIN, P., PITTET, B., GRÖTSCH, J. & DROSTE, H. 2003. The Barremian–Aptian evolution of the eastern Arabian carbonate platform margin (northern Oman). *Journal of Sedimentary Research*, **73**, 756–773.
- HIRSCH, F. 1996. Geology of the southeastern slopes of Mount Hermon. *Current Research – Geological Survey of Israel*, **10**, 22–27.
- HIRSCH, F., FLEXER, A., ROSENFELD, A. & YELLIN-DROR, A. 1995. Palinspastic and crustal setting of the eastern Mediterranean. *Journal of Petroleum Geology*, **18**, 149–170.
- HUSINEC, A. 2001. *Palorbitolina lenticularis* from the Northern Adriatic Region: paleogeographical and evolutionary implications. *Journal of Foraminiferal Research*, **31**, 287–293.
- IMMENHAUSER, A., HILLGÄRTNER, H. & VAN BENTUM, E. 2005. Microbial-foraminiferal episodes in the Early Aptian of the southern Tethyan margin: ecological significance and possible relation to oceanic anoxic event 1a. *Sedimentology*, **52**, 77–99.
- JENKYN, H. C. & WILSON, P. A. 1999. Stratigraphy, paleoceanography, and evolution of Cretaceous Pacific Guyots: relicts from a greenhouse earth. *American Journal of Science*, **299**, 341–392.
- KEELEY, M. L. 1994. Phanerozoic evolution of the basins of northern Egypt and adjacent areas. *Geologische Rundschau*, **83**, 728–742.
- KEMPER, E. 1995. Die Entfaltung der Ammoniten und die Meeresverbindungen im borealen Unter- und Mittel-Apt. In: KEMPER, E. (ed.) *Geologisches Jahrbuch*. Hannover: Schweizerbart'sche Verlagsbuchhandlung, Nägele & Obermiller, 171–199.
- KOTETISHVILI, Z. V. 1970. Stratigraphy and fauna of Colchidites and adjacent horizons of western Georgia [in Russian]. *Akademiya Nauk Grusinskoj SSR Trudy*, **25**, 5–116.
- KUSS, J. & BACHMANN, M. 1996. Cretaceous paleogeography of the Sinai Peninsula and neighbouring areas. *Comptes Rendus de l'Académie des Sciences, Serie II. Sciences de la Terre et des Planetes*, **322**, 915–933.
- LEHMANN, J., HELDT, M., BACHMANN, M. & NEGRA, M. E. H. 2007. Cephalopodenfaunen aus dem Apt (Unterkreide) von Tunesien und Ägypten: Vergleich von Faunen, Fazies und Paläobiogeographie. In: ELICKI, O. & SCHNEIDER, J. W. (eds) *Wissenschaftliche Mitteilungen*. Technische Universität Bergakademie, Freiberg, 78–79.
- LILLO BEVIA, J. 1975. Sobre algunos Hoplitidos del Cretácico inferior del sur de Alicante. *Boletín de la Real Sociedad Española de Historia Natural, Sección Geológica*, **73**, 81–101.
- LUCIANI, V., COBIANCHI, M. & JENKYN, H. C. 2001. Biotic and geochemical response to anoxic events: the Aptian pelagic succession of the Gargano Promontory (southern Italy). *Geological Magazine*, **138**, 277–298.
- LUCIANI, V., COBIANCHI, M. & LUPI, C. 2006. Regional record of a global oceanic anoxic event: OAE1a on the Apulia Platform margin, Gargano Promontory, southern Italy. *Cretaceous Research*, **27**, 754–772.
- MAEDA, H. & SEILACHER, A. 1996. Ammonoid taphonomy. In: LANDMAN, N. H., TANABE, K. & DAVIS, R. A. (eds) *Ammonoid Paleobiology*. Topics in Geobiology, **13**, Plenum Press, New York, 543–578.
- MART, Y., RYAN, W. B. F. & LUNINA, O. V. 2005. Review of the tectonics of the Levant Rift system: the structural significance of oblique continental breakup. *Tectonophysics*, **395**, 209–232.
- MARTINOTTI, G. M. 1993. Foraminiferal evidence of a hiatus between the Aptian and Albian, offshore Northern Sinai. *Journal of Foraminiferal Research*, **23**, 66–75.
- MASSE, J.-P. 1993. Valanginian–Early Aptian carbonate platforms from Provence, southeastern France. In: SIMO, J. A. T., SCOTT, R. W. & MASSE, J.-P. (eds) *Cretaceous Carbonate Platforms*. American Association of Petroleum Geologists, Tulsa, 363–374.
- MASSE, J.-P. 1998. (Coord. U. Cret.). Calcareous algae. In: HARDENBOL, J., JACQUIN, T., FARLEY, M. B., DE GRACIANSKY, P.-C. & VAIL, P. (eds) *Cretaceous Biostratigraphy*. SEPM Special Publication, Tulsa, chart 5.
- MASSE, J.-P., PHILIP, J. & CAMOIN, G. 1995. The Cretaceous Tethys. In: NAIRN, A. E. M., RICOU, L.-E., VRIELYNCK, B. & DERCOURT, J. (eds) *The Tethys Ocean*. Plenum Press, New York, 215–236.
- MASSE, J.-P., FENERCI, M. & PERNARCIC, E. 2003. Palaeobathymetric reconstruction of peritidal carbonates, Late Barremian, Urgonian, sequences of Provence (SE France). *Palaeogeography, Palaeoclimatology, Palaeoecology*, **200**, 65–81.
- MENEGATTI, A. P., WEISSERT, H., BROWN, R. S., TYSON, R. V., FARRIMOND, P., STRASSER, A. & CARON, M. 1998. High-resolution $\delta^{13}\text{C}$ stratigraphy through the early Aptian “Livello Selli” of the Alpine Tethys. *Paleoceanography*, **13**, 530–545.
- MIKHAILOVA, I. A. & BARABOSHKIN, E. J. 2002. *Volgoceratoidea* and *Koeneniceras* – new small-size Lower Aptian heteromorphs from the Ulijanovsk region (Russian Platform). In: SUMMESBERGER, H., HILSTON, K. & DAURER, A. (eds) *Abhandlungen der Geologischen Bundes-Anstalt*. Vienna, 539–553.
- MORSI, A.-M. M. 2006. Aptian ostracodes from Gebel Raghawi (Maghara area) in northern Sinai, Egypt: taxonomic, biostratigraphic and paleobiogeographic contributions. *Revue de Paléobiologie*, **25**, 537–565.
- MOULLADE, M., KUHN, W., BERGEN, J. A., MASSE, J.-P. & TRONCHETTI, G. 1998. Correlation of biostratigraphic and stable isotope events in the Aptian historical stratotype of La Bédoule (southeast France). *Comptes Rendus de l'Académie des Sciences – Serie IIA – Earth and Planetary Science*, **327**, 693–698.
- MOUSTAFA, A. R. 2010. Structural setting and tectonic evolution of North Sinai folds, Egypt. In: HOMBERG, C. & BACHMANN, M. (eds) *Evolution of the Levant Margin and Western Arabia Platform since the Mesozoic*. Geological Society, London, Special Publications, **341**, 37–63.
- MOUSTAFA, A. R. & KHALIL, M. H. 1990. Structural characteristics and tectonic evolution of north Sinai

- fold belts. In: SAID, R. & KENAWY, A. (eds) *Geology of Egypt*. Balkema, Rotterdam, 381–389.
- MOUSTAFA, A. R., KHALIL, M. H., PATTON, T. L. & THOMPSON, T. L. 1990. Structural styles and tectonics of the Sinai Peninsula, Egypt: a field trip guidebook. *Supplementary Material for the 1987 Field Trip*. Egyptian Petroleum Exploration Society.
- MÜCKE, A. 2000. Environmental conditions in the Late Cretaceous African Tethys: conclusions from a microscopic-microchemical study of ooidal ironstones from Egypt, Sudan and Nigeria. *Journal of African Earth Sciences*, **30**, 25–46.
- OGG, J. G., AGTERBERG, F. P. & GRADSTEIN, F. M. 2004. The Cretaceous Period. In: GRADSTEIN, F. M., OGG, J. G. & SMITH, A. G. (eds) *A Geologic Time Scale 2004*. Cambridge University Press, Cambridge, 344–383.
- PITTET, B., VAN BUCHEM, F. S. P., HILLGÄRTNER, H., RAZIN, P., GROTSCH, J. & DROSTE, H. 2002. Ecological succession, palaeoenvironmental change, and depositional sequences of Barremian–Aptian shallow-water carbonates in northern Oman. *Sedimentology*, **49**, 555–581.
- PRICE, G. D. 1999. The evidence and implications of polar ice during the Mesozoic. *Earth Science Reviews*, **48**, 183–210.
- PRICE, G. D. 2003. New constraints upon isotope variation during the early Cretaceous (Barremian–Cenomanian) from the Pacific Ocean. *Geological Magazine*, **140**, 513–522.
- RAWSON, P. F., HOEDEMAEKER, P. J. ET AL. 1999. Report on the 4th International Workshop of the Lower Cretaceous Cephalopod Team (IGCP-Project 362). In: RAWSON, P. F. & HOEDEMAEKER, P. J. (eds) *Proceedings 4th International Workshop of the Lower Cretaceous Cephalopod Team (IGCP-Project 362)*. Scripta Geologica, Special Issue, **3**, 3–13.
- RENARD, M., RAFÉLIS, M. D. ET AL. 2005. Early Aptian $\delta^{13}\text{C}$ and manganese anomalies from the historical Cassis-La Bédoule stratotype sections (S.E. France): relationship with a methane hydrate dissociation event and stratigraphic implications. *Carnets de Géologie/Notebooks on Geology*, **Article 2005/04 (CG2005_A04)**, 1–18.
- ROSENBERG, E. 1960. *Geologische Untersuchungen in den Naftalibergen (am Rande des nördlichsten Teiles der Jordansenke, Israel)*. Mitteilungen aus dem Geologischen Institut der Eidgenössischen Technischen Hochschule und der Universität Zürich, **C80**, 1–180.
- ROSENFELD, A. & HIRSCH, F. 2005. The Cretaceous of Israel. In: HALL, J. K., KRASHENINNIKOV, V. A., HIRSCH, F., BENJAMINI, CH. & FLEXER, A. (eds) *Geological Framework of the Levant. Volume II: The Levantine Basin and Israel*. Historical Productions-Hall, Jerusalem, 393–436.
- ROSENFELD, A., HIRSCH, F. & HONIGSTEIN, A. 1995. Early Cretaceous ostracodes from the Levant. In: RIHA, J. (ed.) *International Symposium on Ostracoda*, **12**. Chapman and Hall, London, 111–121.
- ROSENFELD, A., HIRSCH, F., HONIGSTEIN, A. & RAAB, M. 1998. The palaeoenvironment of Early Cretaceous ostracodes in Israel. In: CRASQUIN-SOLEAU, S., BRACCINI, F. & LETHIERS, F. (eds) *What about Ostracoda!* Bulletin de Centre Recherche et Exploration-Production de Elf-Aquitaine, **Mémoire**, **20**, 179–195.
- ROSS, D. J. 1992. Sedimentology and depositional profile of a Mid-Cretaceous shelf edge rudist reef complex, Nahal Ha'mearot, northwestern Israel. *Sedimentary Geology*, **79**, 161–172.
- SAID, R. 1971. Explanatory notes to accompany the Geological Map of Egypt. *Geological Survey of Egypt*, Papers, 1–123.
- SAINT-MARC, P. 1974. *Etude stratigraphique et micropaléontologique de l'Albien, du Cenomanien et du Turonien du Liban*. Museum National d'Histoire Naturelle, Paris, 342.
- SASS, E. & BEIN, A. 1982. The Cretaceous carbonate platform in Israel. *Cretaceous Research*, **3**, 135–144.
- SCHROEDER, R. 1975. General evolutionary trends in orbitolinas. *Revista Española de Micropaleontología, Núm. especial*, 117–128.
- SCHROEDER, R. & NEUMANN, M. 1985. Les grands Foraminifères du Crétacé moyen de la Région Méditerranéenne. *Geobios, mémoire spéciale*, **7**, 1–160.
- SCHROEDER, R., CLAVEL, B., CHERCHI, A., BUSNARDO, R., CHAROLLAIS, J. & DECROUEZ, D. 2002. Lignées phylétiques d'Orbitolinidés de l'intervalle Hauterivien supérieur – Aptien inférieur; leur importance stratigraphique. *Revue de Paléobiologie, Genève*, **21**, 853–863.
- SCHULZE, F., MARZOUK, A. M., BASSIOUNI, M. A. A. & KUSS, J. 2004. The late Albian–Turonian carbonate platform succession of west-central Jordan: stratigraphy and crises. *Cretaceous Research*, **25**, 709–737.
- SHARIKADZE, M. Z., KAKABADZE, M. V. & HOEDEMAEKER, P. J. 2004. Aptian and Early Albian Douvilleiceratidae, Acanthohoplitidae and Parahoplitidae of Colombia. In: DONOVAN, S. K. (ed.) *Early Cretaceous Ammonites from Colombia*. Scripta Geologica, **128**, 313–514.
- SHARLAND, P. R., ARCHER, R. ET AL. 2001. *Arabian Plate sequence stratigraphy*. Gulf PetroLink, Bahrain, 369.
- SIMMONS, M. D. 1994. Micropalaeontological biozonation of the Kahmah Group (Early Cretaceous), central Oman Mountains. In: SIMMONS, M. D. (ed.) *Micropalaeontology and Hydrocarbon Exploration in the Middle East*. Chapman and Hall, London, 177–219.
- SIMMONS, M. D. & HART, M. B. 1987. The biostratigraphy and microfacies of the Early to mid-Cretaceous carbonates of Wadi Mi'aidin, Central Oman Mountains. In: HART, M. B. (ed.) *Micropalaeontology of Carbonate Environments*. Ellis Harwood, Chichester, 176–207.
- SIMMONS, M. D., WHITTAKER, J. E. & JONES, R. W. 2000. Orbitolinids from Cretaceous sediments of the Middle East – a revision of the F.R.S. Henson and Associated Collection. In: HART, M. B., KAMINSKI, M. & SMART, C. (eds) *Proceedings of the Fifth International Workshop on Agglutinated Foraminifera*, 411–437.
- STAMPFLI, G. M. & BOREL, G. D. 2002. A plate tectonic model for the Paleozoic and Mesozoic constrained by dynamic plate boundaries and restored synthetic oceanic isochrons. *Earth and Planetary Science Letters*, **196**, 17–33.

- STAMPFLI, G. M., BOREL, G., CAVAZZA, W., MOSAR, J. & ZIEGLER, P. 2001. *The Paleotectonic Atlas of the Peritethyan Domain*. European Geophysical Society. CD-ROM, realized by Electronic Publishing & Consulting, Berlin.
- STEBER, T. & BACHMANN, M. 2002. Upper Aptian – Albian rudist bivalves from Northern Sinai, Egypt. *Palaeontology*, **45**, 725–749.
- STRASSER, A., CARON, M. & GJERMENI, M. 2001. The Aptian, Albian and Cenomanian of Roter Sattel, Romandes Prealps, Switzerland: a high-resolution record of oceanographic changes. *Cretaceous Research*, **22**, 173–199.
- VAIL, P. R., AUDEMARD, F., BOWMAN, S. A., EISNER, P. N. & PEREZ-CRUZ, C. 1991. The stratigraphic signatures of tectonics, eustasy and sedimentology – an overview. In: EINSELE, G., RICKEN, W. & SEILACHER, A. (eds) *Cycles and Events in Stratigraphy*. Springer, Berlin, Heidelberg, 617–659.
- VAN BUCHEM, F., CASANOVA, J. *ET AL.* 2001. Southern Tethys platform evolution and chemostratigraphy during the Middle Cretaceous (Southeastern Arabian Plate, N. Oman and U.A.E.). In: WORTMANN, U. & FUNK, H.-P. (eds) *IAS-2001*, 21st Meeting, Davos, Abstracts, 167.
- VAN BUCHEM, F. S. P., PITTET, B. *ET AL.* 2002. High-resolution sequence stratigraphic architecture of Barremian/Aptian carbonate systems in Northern Oman and the United Arab Emirates (Kharai and Shuaiba Formations). *GeoArabia*, **7**, 461–500.
- WEISSERT, H. & ERBA, E. 2004. Volcanism, CO₂ and palaeoclimate: a Late Jurassic-Early Cretaceous carbon and oxygen isotope record. *Journal of the Geological Society, London*, **161**, 695–702.
- WEISSERT, H., LINI, A., FÖLLMI, K. B. & KUHN, O. 1998. Correlation of Early Cretaceous carbon isotope stratigraphy and platform drowning events: a possible link? *Palaeogeography, Palaeoclimatology, Palaeoecology*, **137**, 189–203.
- WESTERMANN, G. E. G. 1996. Ammonoid life and habit. In: LANDMAN, N. H., TANABE, K. & DAVIS, R. A. (eds) *Ammonoid Paleobiology*. Topics in Geobiology. New York: Plenum Press, 607–707.
- WISSLER, L., FUNK, H. & WEISSERT, H. 2003. Response of Early Cretaceous carbonate platforms to changes in atmospheric carbon dioxide levels. *Palaeogeography, Palaeoclimatology, Palaeoecology*, **200**, 187–205.
- YOUNG, K. 1974. Lower Albian and Aptian (Cretaceous) ammonites of Texas. *Geoscience and Man*, **3**, 175–228.